Soil Biology and Biochemistry 148 (2020) 107871

Contents lists available at ScienceDirect

Soil Biology and Biochemistry

journal homepage: http://www.elsevier.com/locate/soilbio

# A soil microbial model to analyze decoupled microbial growth and respiration during soil drying and rewetting

Albert C. Brangarí [a,b,*], Stefano Manzoni [c,d], Johannes Rousk [b]

[a] Centre for Environmental and Climate Research (CEC), Lund University, Lund, Sweden
[b] Microbial Ecology, Department of Biology, Lund University, Lund, Sweden
[c] Department of Physical Geography, Stockholm University, Stockholm, Sweden
[d] Bolin Centre for Climate Research, Stockholm, Sweden

ARTICLE INFO

*Keywords:*
Birch effect
Modeling
Moisture
Carbon dynamics
Carbon-use efficiency
Microbial mechanisms
"EcoSMMARTS" (the ecological version of a soil microbial model to account for responses to stress)

ABSTRACT

Soils are continuously exposed to cycles of drying and rewetting (D/RW), which drive pronounced fluctuations in soil carbon (C) fluxes. These C dynamics are characterized by a decoupled behavior between microbial biomass synthesis (growth) and $CO_2$ production (respiration). In general, respiration rates peak shortly after RW and subsequently decrease, while the growth peaks lag several hours behind. Despite the significance of these dynamics for the soil C budget and the global C cycle, this feature has so far been overlooked in biogeochemical models and the underlying mechanisms are still unclear. We present a new process-based soil microbial model that incorporates a wide range of physical, chemical and biological mechanisms thought to affect D/RW responses. Results show that the model is able to capture the respiration dynamics in soils exposed to repeated cycles of D/RW, and also to single events in which moisture was kept constant after RW. In addition, the model reproduces, for the first time, the responses of microbial growth to D/RW. We have identified the C accumulation during dry periods, the drought-legacy effect on the synthesis of new biomass, and osmoregulation as the strongest candidate mechanisms to explain these C dynamics. The model outputs are further compared to earlier process-based models, highlighting the advances generated by the new model. This work thus represents a step towards unravelling the microbial responses to drought and rainfall events, with implications for our understanding of C cycle and C sequestration in soils.

## 1. Introduction

Soils represent the largest terrestrial pool of organic carbon (C), so that any change in soil C stocks may transfer substantial amounts of C into or out of the atmosphere (Lee et al., 2004; Reichstein et al., 2013; Rustad et al., 2000). The input-output fluxes in soils are regulated by complex soil microbial processes such as litter decomposition, respiration, and sequestration; which, in turn, are driven by hydro-climatic variables. The marked temporal variability of hydro-climatic conditions, where extended periods of drought are followed by rainfall events, drive pronounced fluctuations in biogeochemical fluxes (Birch, 1958; Homyak et al., 2018; Jarvis et al., 2007; Schimel et al., 2007). However, the mechanisms that generate these responses remain unresolved (Kim et al., 2012; Manzoni et al., 2012b). The use of process-based models of soil organic carbon (SOC) can help to disentangle the underlying mechanisms and feedbacks governing the soil responses to moisture fluctuations.

Water is essential for the proliferation of any form of life, and soil microorganisms are not the exception. The availability of water influences the microbial performance and fitness, which in turn regulate the nature of most of the processes taking place in soils (Jenny, 1980; Or et al., 2007a; Schimel and Schaeffer, 2012). Soil water content controls the physiological stress cells are exposed to and the cellular accessibility to resources (Carbone et al., 2011; Fierer and Schimel, 2002; Manzoni et al., 2012a; Or et al., 2007b). In dry environments, water stressed communities are expected to exhibit low C-use efficiencies (CUE), since they have to shift their allocation of resources from growth to survival (Brangarí et al., 2018; Manzoni et al., 2012b; Schimel et al., 2007; Schimel, 2018). Furthermore, natural soils are not exposed to constant moisture conditions but to successive cycles of drying-rewetting (D/RW), which expose microorganisms to variable environmental conditions. The microbial response to moisture fluctuations is characterized

* Corresponding author. Microbial Ecology, Department of Biology, Lund University, Lund, Sweden.
*E-mail address:* albert.brangari@biol.lu.se (A.C. Brangarí).

https://doi.org/10.1016/j.soilbio.2020.107871
Received 27 January 2020; Received in revised form 24 May 2020; Accepted 26 May 2020
Available online 1 June 2020

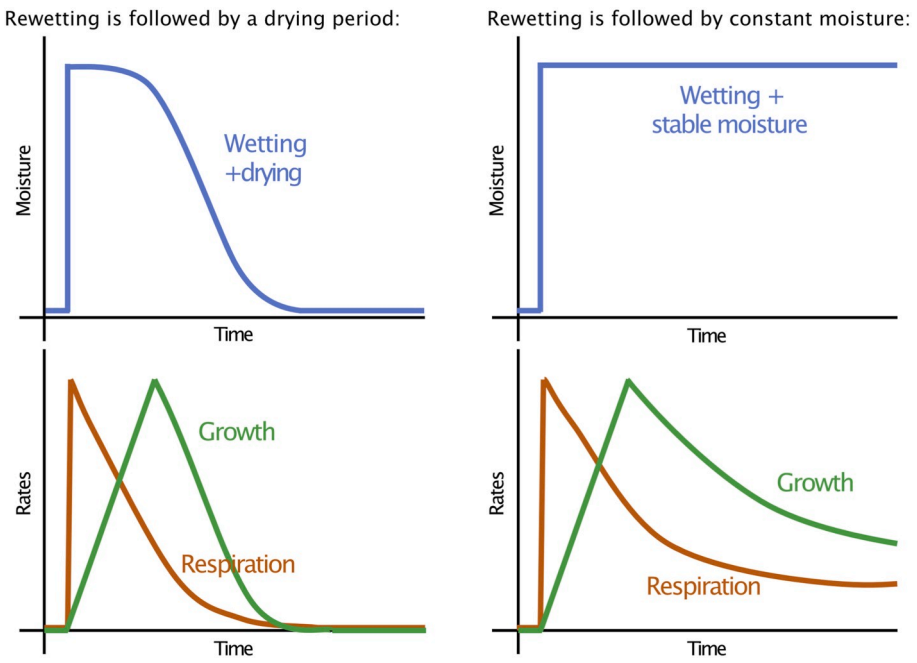


**Fig. 1.** Conceptual representation of the patterns of microbial growth and respiration after rewetting of a dry soil reported by the literature. Two different types of experiments are depicted: in the left panels, rewetting is followed by a drying period (as in Barnard et al., 2015; Jarvis et al., 2007; Miller et al., 2005; Tiemann and Billings, 2011), while in the right panels, soil moisture is kept at a constant level after rewetting, which is the most commonly used experimental procedure (as in, e.g., Chase and Gray, 1957; Chowdhury et al., 2011; de Nijs et al., 2018; De Nobili et al., 2006; Griffiths and Birch, 1961; Kieft et al., 1987; Meisner et al., 2013; Placella et al., 2012; Slessarev et al., 2020; Wu et al., 1997). While in all cases a rapid peak in respiration is accompanied by a delayed response in growth rates, the timing of these processes and the post-perturbation rates (steady-state) differ depending on the resilience of the system and on the length and characteristics of the moisture disturbance.

by a disconnected behavior between microbial biomass synthesis (growth) and $CO_2$ production (respiration) (e.g., Blazewicz et al., 2014; de Nijs et al., 2018; Göransson et al., 2013; Meisner et al., 2017, 2013; Tiemann and Billings, 2011; Zheng et al., 2019). Typically, respiration rates peak rapidly upon RW and then decrease exponentially, even though the soil moisture is still high (Fig. 1). However, the growth of the microbial community starts increasing linearly after RW and reaches its peak only after several hours. Such decoupled respiration and growth dynamics result in a very low CUE after RW that gradually recover to higher values.

Even though current SOC models can adequately reproduce the respiration patterns (e.g., Evans et al., 2016; Lawrence et al., 2009; Li et al., 2010; Slessarev and Schimel, 2020), the dynamics of microbial growth and the drivers and the characteristics of the respiration and growth responses have been overlooked or have been treated implicitly. For example, respiration pulses have been described via empirical factors (e.g., Li et al., 2010), which capture patterns in the data but neglect the underlying mechanisms. Other approaches described soil moisture as a regulator of microbial activity (e.g., Maggi and Porporato, 2007) or mineralization rates (e.g., Bauer et al., 2008), where both growth and respiration were merely a consequence of them. Several contributions developed more complex process-based models to mechanistically reproduce SOC dynamics during D/RW. For instance, Evans et al. (2016) and Lawrence et al. (2009) explored the limitations in soil diffusion and microbial activity, and Slessarev and Schimel (2020) evaluated the dynamic contribution of different C sources, but respiration and growth were kept synchronized. Salazar et al. (2018) studied the C implications of dormancy distinguishing between growth and respiration, and Brangarí et al. (2018) and Manzoni et al. (2014) explored complex physio-morphological adaptations to withstand water stress. However, no current models could capture the strong growth-respiration decoupling recently uncovered (by, e.g., Göransson et al., 2013; Iovieno and Bååth, 2008), suggesting that some important mechanisms are still missing or improperly described.

Both empirical evidence and theoretical work have identified potential drivers of D/RW-induced microbial dynamics. On the one hand, large respiration rates upon RW suggest that C accumulated during the preceding dry period becomes available, sourced from e.g. dead microbial biomass (Blazewicz et al., 2014; Khan et al., 2016), exoenzymatic activity (Romaní et al., 2008; Vetter et al., 1998), polymeric substances (Brangarí et al., 2018; Flemming and Wingender, 2010), previously physically protected soil aggregates (Fierer and Schimel, 2003; Navarro-García et al., 2012), or from soil pores that were hydrologically disconnected during drought (Manzoni et al., 2016). On the other hand, the contrasting patterns of respiration and growth suggest the existence of processes that are regulated as a response to environmental stress and the legacy of drought (de Nijs et al., 2018; Göransson et al., 2013). Microbial processes such as osmoregulation (Kakumanu et al., 2013; Warren, 2016), dormancy (Blagodatskaya and Kuzyakov, 2013; Lennon and Jones, 2011), and enzyme production (Kirchman, 2013; Schimel and Weintraub, 2003) result in a variable allocation of C with different contributions to respiration and growth. Recent studies have also demonstrated the existence of extracellular mechanisms contributing to SOC mineralization that are not associated with metabolism (Fraser et al., 2016; Kéraval et al., 2018). Essentially, the responses to D/RW are the result of the feedbacks between soil moisture and several bio-physical processes, which end up defining C availability, resource allocation, microbial activity, cell mortality, and the activation of a complex range of survival strategies.

In this work, we incorporated the mechanisms proposed in the literature and formalized them via a new process-based soil microbial model "EcoSMMARTS" (the Ecological version of a Soil Microbial Model to Account for Responses To Stress). The result is a tool that can be used to better understand the mechanisms and feedbacks governing the soil

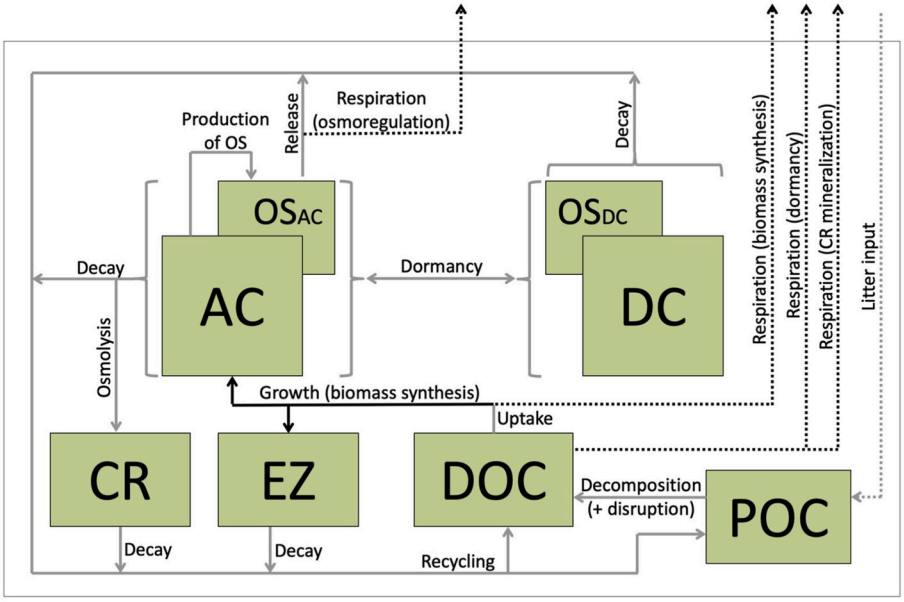


**Fig. 2.** Schematic representation of the model EcoSMMARTS. Soil organic carbon is differentiated into eight compartments (green boxes): particulate organic carbon (POC), dissolved organic carbon (DOC), active cells (AC), dormant cells (DC), extracellular enzymes (EE), intracellular osmolytes ($OS_{AC}$ and $OS_{DC}$), and cell residues (CR). The arrows specify the direction of carbon fluxes between pools (solid lines) and sources or losses from the soil system (dotted lines). The lines marked in black indicate that fluxes contribute to either growth (solid) or respiration (dotted). (For interpretation of the references to colour in this figure legend, the reader is referred to the Web version of this article.)

responses to changes in moisture and their implications for the soil C cycle. We evaluated the capability of the model to: i) capture the respiration dynamics in repeated D/RW cycles in Miller et al. (2005), ii) reproduce the respiration-growth response patterns responding to a single RW event after which moisture is kept constant, and iii) elucidate the mechanisms driving the soil response to hydro-climatic forcing required for i) and ii). The model outputs were additionally compared to a widely used set of models by Lawrence et al. (2009).

## 2. Materials and methods

### 2.1. Model structure of EcoSMMARTS

The SOC is differentiated into eight compartments: particulate organic carbon (POC), dissolved organic carbon (DOC), active cells (AC), dormant cells (DC), extracellular enzymes (EE), intracellular osmolytes ($OS_{AC}$ and $OS_{DC}$), and cell residues (CR). The POC compartment consists of plant materials and microbial byproducts available for decomposition. POC cannot be used directly by microorganisms, without first being transformed into simpler compounds, here represented as DOC. The DOC compartment accounts for dissolved compounds considered labile. Besides products from POC decomposition, DOC is derived from products of microbial decay and extracellular osmolytes. Soil microorganisms are classified according to their current level of functionality, distinguishing between active cells and dormant cells. Enzymes produced by active cells are the biological catalysts responsible for POC decomposition. The osmolytes are denoted as $OS_{AC}$ and $OS_{DC}$ based on their location either in active or dormant cells, respectively. Finally, CR are microbial residues catabolically active but unable to grow, which sustain extracellular mineralization (details will follow in Section 2.7).

The model incorporates the wide range of processes and mechanisms governing microbial responses to soil moisture changes, including (Fig. 2): POC decomposition (POC→DOC), microbial uptake and C investment in biomass (DOC→AC + EE), dormancy (inactivation vs reactivation; AC↔DC), recycling of microbial decay products (biomass→DOC + POC), osmoregulation (production and release of osmolytes; AC→OS→DOC), and C mineralization by cell residues (DOC→$CO_2$). The synthesis of biomass, osmoregulation and dormancy also contribute to respiration (→$CO_2$) (Fig. 2). All process rates are mediated according to the microbial needs under specific environmental conditions, where soil moisture plays a key role (Sections 2.2-2.8 and summarized in Table 1). The model is spatially lumped and the dynamics are interpreted at the minute time scale. The mass balance equations representing the dynamics of the C compartments can be written as,

$$\frac{d\overline{POC}}{dt} = \underbrace{L}_{\text{Litter input}} - \underbrace{D^{POC}}_{\text{POC decomposition}} + \underbrace{(1-\lambda_r)\left[K^{AC} + (1-\lambda_z)K_s^{AC} + K^{DC} + K^{CR} + K^{EE}\right]}_{\text{Recycling of decay products}} \quad (1)$$

$$\frac{d(\theta_w\overline{DOC})}{dt} = \underbrace{D^{POC}}_{\text{POC decomposition}} - \underbrace{U^{AC}}_{\text{Uptake by AC}} - \underbrace{C^{CR}}_{\text{CR mineralization}} + \underbrace{\lambda_r\left[K^{AC} + (1-\lambda_z)K_s^{AC} + K^{DC} + K^{CR} + K^{EE}\right]}_{\text{Recycling of decay products}} - \underbrace{z_r R^{DC}}_{\text{Dormancy costs}} + \underbrace{w_b\overline{OS_{AC}}\left(K^{AC} + K_s^{AC}\right) + w_b\overline{OS_{DC}}K^{DC}}_{\text{Recycling of OS (cell decay)}} + \underbrace{y_{os}E^{OS}}_{\text{Recycling of OS (osmoregulation)}} - \underbrace{S^{DOC}}_{D/RW} \quad (2)$$

$$\frac{d\overline{AC}}{dt} = \underbrace{y^*(1-\lambda^*)U^{AC}}_{AC\ synthesis} - \underbrace{I^{AC}}_{Inactivation} + \underbrace{R^{DC}}_{Reactivation} - \underbrace{P^{OS}}_{OS\ production} - \underbrace{K^{AC}}_{AC\ natural\ decay} - \underbrace{K_s^{AC}}_{AC\ decay\ by\ stress} \tag{3}$$

$$\frac{d\overline{DC}}{dt} = \underbrace{I^{AC}}_{Inactivation} - \underbrace{R^{DC}}_{Reactivation} - \underbrace{K^{DC}}_{DC\ decay} \tag{4}$$

$$\frac{d\overline{CR}}{dt} = \underbrace{\lambda_z K_s^{AC}}_{Osmolysis} - \underbrace{K^{CR}}_{CR\ decay} \tag{5}$$

$$\frac{d(\theta_w\overline{EE})}{dt} = \underbrace{y^*\lambda^* U^{AC}}_{EE\ synthesis} - \underbrace{K^{EE}}_{EE\ decay} - \underbrace{S^{EE}}_{D/RW} \tag{6}$$

$$\frac{d(\theta_{AC}\,\overline{OS_{AC}})}{dt} = \underbrace{P^{OS}}_{OS\ production} - \underbrace{E^{OS}}_{OS\ elimination} + \underbrace{w_b\overline{OS_{DC}}R^{DC}}_{OS\ reactivation} - \underbrace{w_b\overline{OS_{AC}}I^{AC}}_{OS\ inactivation} - \underbrace{w_b\overline{OS_{AC}}\left(K^{AC}+K_s^{AC}\right)}_{OS\ release\ (AC\ decay)} \tag{7}$$

$$\frac{d(\theta_{DC}\,\overline{OS_{DC}})}{dt} = \underbrace{-w_b\overline{OS_{DC}}R^{DC}}_{OS\ reactivation} + \underbrace{w_b\overline{OS_{AC}}I^{AC}}_{OS\ inactivation} - \underbrace{w_b\overline{OS_{DC}}K^{DC}}_{OS\ release\ (DC\ decay)} \tag{8}$$

The concentrations of POC, AC, DC, and CR are defined as mass of C per unit volume of soil ($\overline{POM}$, $\overline{AC}$ $\overline{DC}$, and $\overline{CR}$, respectively), but the dissolved compounds are expressed in mass per unit volume of soil water ($\overline{DOC}$ and $\overline{EE}$), or mass per unit volume of cell ($\overline{OS_{AC}}$ and $\overline{OS_{DC}}$). The soil moisture content ($\theta_w$), and the volume of water in active ($\theta_{AC}$) and dormant cells ($\theta_{DC}$) allow writing the equations for the dissolved compounds and cellular constituents in terms of mass of C per unit volume of soil. $w_b$ is the cell-density conversion coefficient (Eq. (31) and Eq. (32)) and is used to determine the influence of the processes targeting cells (e.g., decay, inactivation, reactivation) on the pools of osmolytes. All mass balance equations are written then in terms of compartment C-mass [mg] per unit volume of soil [$cm^3$] and per unit time [min]. The full description of the model equations and their formulations are provided in Appendix 3, whereas the modeling of soil moisture (and water potential) and its effect on soil processes can be found in Appendixes 1 and 2, respectively. A MATLAB file ("RunEcoSMMARTS_Miller.m") with the model and the code to obtain the results in Section 4.1 (as an example) is available at https://github.com/Brangari/EcoSMMARTS.git.

### 2.2. Effects of soil moisture on modelled processes

Most processes and SOC compartments in this model are affected by soil water content directly, indirectly, or both (Table 1). The impact on soil moisture and water potential on these processes is described using six rate modifiers: $\chi_\tau$, $\chi_a$, $\chi_{os}^s$, $\chi_{os}^r$, $\Gamma_s$, and $\Gamma_m$ (see Appendix 2 for mathematical definition and details).

The coefficient of tortuosity $\chi_\tau$ (Eq. (16)) describes the effect of twists and turns of the water-filled pore space, which subsequently determines the ease with which enzymes reach the sites of depolymerization and, therefore, the decomposition rates. The $\chi_\tau$ is a continuous function of soil moisture, decreasing to zero when $\theta_w = 0$. As soil dries, hydraulic connectivity breaks down below the so-called percolation point and advective and diffusive transport stops. However, at the small spatial scales at which microbial processes operate, some degree of connectivity remains (Manzoni and Katul, 2014), allowing us to use a continuous $\chi_\tau$ function. The water-stress coefficient $\chi_a$ (Eq. (17)) describes how the current moisture content affects the microbial performance, determining the potential of C uptake and the rate of cell inactivation. This empirical rate modifier takes into account both physical and biological aspects of water stress on microorganisms. $\chi_a$ is assumed to be highest at around 50% water holding capacity (WHC), which represent optimal conditions, corresponding to −348 cm (c. −34 KPa), and to decrease at lower or higher soil moisture respectively due to reduced substrate availability and physiological stress (when drier), and oxygen diffusion limitation (when wetter). $\chi_{os}^r$ and $\chi_{os}^s$ represent two aspects of osmoregulation. The coefficient of osmoregulation $\chi_{os}^r$ (Eq. (22)) is the indicator of the needs for production/elimination of osmolytes. In contrast, the coefficient of osmotic stress $\chi_{os}^s$ (Eq. (21)) is an indicator of the physiological stress experienced by cells when the osmotic potential (osmolyte concentration) mismatched to its environment (see Appendix 2 for details). Finally, the drought-legacy effects, or the "memory" of the preceding conditions, are represented by a function that keeps track of duration and intensity of previous dry conditions (Eq. (18)). This function affects the responses of both microorganisms ($\Gamma_m$) and soil structure ($\Gamma_s$). The former controls the efficiency of C conversion to growth (influencing the CUE of biomass synthesis; Eq. (9)) and the rate at which cells recover from dormancy (Eq. (28)), whereas $\Gamma_s$ regulates the disruption of soil aggregates. A detailed description of the processes involved is presented in Sections 2.3-2.8.

### 2.3. Carbon availability

The rates of POC decomposition ($D^{POC}$) are modulated by moisture content through $\chi_\tau$. Despite being largely reduced, $D^{POC}$ continues even under very dry conditions since enzymatic activity may persist in microhabitats where water is still held (Chau et al., 2011; Or et al., 2007b). The capacity of decomposition is also influenced by the legacy of drought episodes on soil structure (through $\Gamma_s$). Drought and severe shifts in hydration promote the disruption of aggregates, releasing organic substrates from physical protection and promoting increased decomposition rates (Fierer and Schimel, 2003; Navarro-García et al., 2012). Besides these inputs from POC, the DOC pool is fed by products of microbial origin. A fraction $\lambda_r$ of decayed biomass (from AC, DC, EE, and CR), the OS contained in decayed cells, and a fraction $y_{os}$ of the OS released during osmoregulation ($E^{OS}$) remain in the soil system as DOC. The remaining decayed biomass ($1-\lambda_r$) becomes POC, while the remaining osmolytes ($1-y_{os}$) are used as energy sources during osmoregulation.

### 2.4. Carbon uptake and biomass synthesis

The microbial uptake rate ($U^{AC}$) is modulated according to the microbial demand for resources and by the influence of moisture on microbial performance (via $\chi_a$). Yet, not all the C taken up is efficiently used. The fraction of C that is eventually transformed into biomass (not lost by respiration) also changes over time and is known as the effective yield coefficient of C uptake or the CUE of biomass synthesis:

$$y^* = y\Gamma_m\left(1-\min\left(1,\chi_{os}^s\right)\right) \tag{9}$$

where $y$ is the yield coefficient of C uptake at optimal conditions. Increasing osmotic stress and drought-legacy effects cause $\chi_{os}^s$ to increase and $\Gamma_m$ to decrease, respectively, thereby lowering the efficiency of the process. The C that is not respired is allocated to the synthesis of new AC or EE (Eq. (3) and Eq. (6)). In turn, C allocation to enzymes ($\lambda^*$; Eq. (26)) is reduced when the enzymatic concentration is high enough to promote efficient foraging.

### 2.5. Osmoregulation

Microorganisms may modulate their intracellular concentration of osmolytes to regulate the physiological stress experienced during D/RW

**Table 1**
List of state variables, processes rates, and parameters. Direct dependence of process rates on water availability and carbon pools status. The influence of moisture is defined through the coefficients of water-stress ($\chi_a$), tortuosity ($\chi_t$), osmotic stress ($\chi^s_{os}$), osmotic regulation ($\chi^r_{os}$), and drought-legacy on soils ($\Gamma_s$) and or microorganisms ($\Gamma_m$).

| Symbol | Description | Units | Dependence of rates and rate modifiers on: | |
|---|---|---|---|---|
| | | | Soil moisture | C pools |
| **State variables** | | | | |
| $\overline{AC}$ | Concentration of active cells per unit volume of soil | mg/cm$^3$ | | |
| $\overline{CR}$ | Concentration of cell residues per unit volume of soil. Residues from lysed organisms unable to grow | mg/cm$^3$ | | |
| $\overline{DC}$ | Concentration of dormant cells per unit volume of soil. Reversible state of inactivity | mg/cm$^3$ | | |
| $\overline{DOC}$ | Concentration of dissolved organic carbon per unit volume of water | mg/cm$^3$ | | |
| $\overline{EE}$ | Concentration of extracellular enzymes per unit volume of water | mg/cm$^3$ | | |
| $\overline{OS_{AC}}$ | Concentration of osmolytes per unit volume of active cells | mg/cm$^3$ | | |
| $\overline{OS_{DC}}$ | Concentration of osmolytes per unit volume of dormant cells | mg/cm$^3$ | | |
| $\overline{POC}$ | Concentration of particulate organic carbon per unit volume of soil | mg/cm$^3$ | | |
| $t$ | Time | min | | |
| $\theta_w$ | Soil moisture (water content per unit volume of soil) | – | | |
| **Rates** | | | | |
| $C^{CR}$ | Mineralization of DOC by cell residues. Catabolic use of carbon by extracellular microbial residues | mg/cm$^3$/min | $\chi_a$ | $\overline{CR}$, $\overline{DOC}$ |
| $D^{POC}$ | Decomposition of particulate carbon. Shifts in hydration cause increased rates by the disruption of soil aggregates | mg/cm$^3$/min | $\chi_t$, $\Gamma_s$ | $\overline{EE}$, $\overline{POC}$ |
| $E^{OS}$ | Rate of osmolytes elimination to compensate osmotic shock upon rewetting | mg/cm$^3$/min | $\chi^r_{os}$ | $\overline{AC}$, $\overline{OS_{AC}}$ |
| $I^{AC}$ | Rate of inactivation of active cells | mg/cm$^3$/min | $\chi_a$ | $\overline{AC}$, $\overline{DOC}$ |
| $L$ | Rate of external supply of POC | mg/cm$^3$/min | | |
| $P^{OS}$ | Rate of osmolytes production to compensate osmotic stress under dry conditions | mg/cm$^3$/min | $\chi^r_{os}$ | $\overline{AC}$, $\overline{OS_{AC}}$ |
| $R^{DC}$ | Reactivation of dormant cells | mg/cm$^3$/min | $\Gamma_m$ | $\overline{DC}$, $\overline{DOC}$ |
| $K^{AC}$ | Rate of decay of active cells (normal turnover) | mg/cm$^3$/min | | $\overline{AC}$ |
| $K^{AC}_s$ | Rate of decay of active cells (by stress) | mg/cm$^3$/min | $\chi^s_{os}$ | $\overline{AC}$ |
| $K^{DC}$ | Rate of decay of dormant cells | mg/cm$^3$/min | | $\overline{DC}$ |
| $K^{EE}$ | Rate of decay of enzymes | mg/cm$^3$/min | | $\overline{EZ}$ |
| $K^{CR}$ | Rate of decay of cell residues | mg/cm$^3$/min | | $\overline{CR}$ |
| $U^{AC}$ | Rate of uptake of dissolved organic carbon | mg/cm$^3$/min | $\chi_a$ | $\overline{AC}$, $\overline{DOC}$ |
| **Parameters** | | | | |
| $t_{m,m}$ | Memory duration for microorganisms | min | | |
| $t_{m,s}$ | Memory duration for soils | min | | |
| $w_b$ | Cell-density conversion coefficient | cm$^3$/mg | | |
| $y_{os}$ | Coefficient of osmolyte recycling. Efficiency of the osmoregulation process | – | | |
| $y$ | Yield coefficient of carbon uptake | – | | |
| $y^*$ | Effective yield coefficient of carbon uptake. CUE of biomass synthesis | – | $\Gamma_m$ | $\overline{OS_{AC}}$ |
| $z_r$ | Coefficient of reactivation costs. Defines the carbon respired associated with dormancy | – | | |
| $\theta_{AC}$ | Volume of water in active cells per unit volume of soil | – | | $\overline{OS_{AC}}$ |
| $\theta_{DC}$ | Volume of water in dormant cells per unit volume of soil | – | | $\overline{OS_{DC}}$ |
| $\lambda_r$ | Coefficient of recycling | – | | |
| $\lambda_z$ | Coefficient of cell residues permanence | – | | |
| $\lambda^*$ | Effective coefficient of allocation | – | | $\overline{EE}$ |

(as in Manzoni et al., 2014). When soils dry, their water potential decreases and this decrease must be compensated through the production of osmolytes ($P^{OS}$). These products must then be rapidly eliminated ($E^{OS}$) at RW to avoid cell lysis. Active cells that do not efficiently regulate the osmolyte concentration are affected by low CUE in biomass synthesis (Eq. (9)) and larger rates of cellular lysis (Eq. (38)), whereas dormant cells are 'protected' from osmotic stress. The dynamics of OS are sensitive to processes affecting the cells in which they are contained, i.e., inactivation and reactivation induce fluxes of OS ($OS_{AC}$ and $OS_{DC}$) between AC and DC, and those OS in decayed cells are automatically released to the environment and transformed into DOC. In the model, osmolytes are synthesized from active cell internal resources (not DOC), and the energy required during osmoregulation entails respiration costs ($(1 - y_{os})E^{OS}$).

### 2.6. Dormancy

The switch between active and inactive (dormant) cell states is described by means of two opposed sub-processes. Inactivation ($I^{AC}$) and reactivation ($R^{DC}$) are governed by the suitability of the environmental conditions. Unlike models that only considered the substrate dependence of dormancy (e.g., Konopka, 2000; Wang et al., 2014), the microbial dormancy in our model is also affected by the influence of soil moisture. The current water content determines the overall microbial performance, which may promote a shift to dormancy (by means of $\chi_a$). The recovery of cell functionality also depends on the duration and

**Table 2**
List of parameters and values used in the EcoSMMARTS simulations.

| Parameter | Description | Value | Units | Notes and refs. |
|---|---|---|---|---|
| $AC_{ini}$ | Initial concentration of AC | 0.7 | mg/cm$^3$ | Active pool in Lawrence et al. (2009) |
| $CR_{ini}$ | Initial concentration of CR | 0 | mg/cm$^3$ | Assumed. Large values alter the patterns of the response |
| $d_1$ | Unit converter coefficient | $10^{-4}$ | J/cm$^4$ | Approximation to adjust the units in the Van't Hoff relation (Eq. (20)) |
| $d_2$ | Molecular weight of a representative osmolyte | $6 \times 10^4$ | mg/mol | A representative osmolyte contains five carbon atoms (Manzoni et al., 2014) |
| $DC_{ini}$ | Initial concentration of DC | 0.7 | mg/cm$^3$ | DC fraction can be up to 60% (Blagodatskaya and Kuzyakov, 2013). Assumed here 50% |
| $(\theta_w\overline{DOC})_{ini}$ | Initial mass of DOC | 0.05 | mg/cm$^3$ | Bio-available C in Lawrence et al. (2009) |
| $DOC_k$ | Half-saturation constant of DOC | 5 | mg/cm$^3$ | Assumed |
| $EE_{ini}$ | Initial concentration of EE | $6 \times 10^{-3}$ | mg/cm$^3$ | Brangarí et al. (Brangarí et al., 2018) |
| $EE_k$ | Half-saturation constant of EE | $6 \times 10^{-4}$ | mg/cm$^3$ | Assumed equal to $EE_{ini}/10$ to avoid initial EE shortage |
| $k_{AC}$ | Constant rate of decay for AC | $1 \times 10^{-6}$ | 1/min | Calibrated |
| $k^s_{AC}$ | Constant rate of decay for AC under stress | $1 \times 10^{-5}$ | 1/min | Assumed equal to $k_{AC} \times 10$ |
| $k_{CR}$ | Constant rate of decay for CR | $1 \times 10^{-6}$ | 1/min | Assumed equal to $k_{AC}$ |
| $k_{DC}$ | Constant rate of decay for DC | $1 \times 10^{-7}$ | 1/min | Assumed equal to $k_{AC}/10$ (Brangarí et al., 2018) |
| $k_{EE}$ | Constant rate of decay for EE | $1 \times 10^{-6}$ | 1/min | Assumed equal to $k_{AC}$ (Brangarí et al., 2018) |
| $m_d$ | Coefficient of aggregate disruption. The potential effect of disruption is $m_d$ times that of the base decomposition | 2 | – | Calibrated |
| $n$ | Empirical coefficient of the van Genuchten's WRC | 1.3824 | – | From calibration of Miller's data (personal communication) |
| $OS_{ini}$ | Initial concentration of $OS_{AC}$ and $OS_{DC}$ | Eq. (23) | mg/cm$^3$ | Initial effective osmoregulation is assumed |
| $OS^{max}_{eq}$ | Maximum $\overline{OS_{AC}}$ in microbial communities | Eq. (20) | mg/cm$^3$ | Van't Hoff relation assuming that the minimum water potential that can be compensated through osmoregulation is $\psi_{M.os}$ |
| $POC_{ini}$ | Initial concentration of POC | 15 | mg/cm$^3$ | Assumed equal to 1% of soil's mass (Brangarí et al., 2018) |
| $R$ | Gas constant value | 8.314 | J/mol/K | Known |
| $t_{m,m}$ | Memory duration for microorganisms | 4320 | min | Assumed equal to 3 days |
| $t_{m,s}$ | Memory duration for soils | 14400 | min | Assumed equal to 10 days |
| $T$ | Temperature | 298.15 | K | Assumed at 25 °C |
| $w_b$ | Volume of water per unit dry C-mass of cell | $1.4 \times 10^{-3}$ | cm$^3$/mg | Manzoni et al. (2014) |
| $y$ | Yield coefficient of carbon uptake | 0.7 | – | Assumed |
| $y_{os}$ | Yield coefficient of OS elimination | 0.6 | – | Calibrated |
| $y^*$ | Effective yield coefficient of carbon uptake | Eq. (9) | – | |
| $z_r$ | Yield coefficient of reactivation | $1 \times 10^{-2}$ | – | Calibrated |
| $\alpha$ | Empirical coefficient of the van Genuchten's WRC | 0.0172 | 1/cm | From calibration of Miller's data (personal communication) |
| $\gamma_\tau$ | Shape parameter in the coefficient of tortuosity | 1.8 | – | Hamamoto et al. (2010) |
| $\Gamma_m$ | Coefficient of drought-legacy on microorganisms | Eq. (18) | – | Using $t_{m,m}$ |
| $\Gamma_s$ | Coefficient of drought-legacy on soils | Eq. (18) | – | Using $t_{m,s}$ |
| $\lambda_{EE}$ | Coefficient of carbon allocation diverted towards EE | 0.01 | – | Brangarí et al. (Brangarí et al., 2018) |
| $\lambda_r$ | Coefficient of recycling | 0.5 | – | Assumed |
| $\lambda_z$ | Coefficient of cell residues permanence | 0.8 | – | Assumed |
| $\lambda^*$ | Effective coefficient of carbon allocation | Eq. (26) | – | |
| $\theta_{AC}$ | Volume of water in active cells | Eq. (31) | – | |
| $\theta_{DC}$ | Volume of water in dormant cells | Eq. (32) | – | |
| $\theta_{fc}$ | Water content at the field capacity | Eq. (14) | – | Water content estimated at $\psi_{fc}$ |
| $\theta_s$ | Saturated water content | 0.32 | – | From Miller's data (personal communication) |
| $\theta_r$ | Residual water content | 0 | – | From Miller's data (personal communication) |
| $\theta^*_w$ | Water content matching point in the modified Webb's equation | Eq. (15) | – | Based on Webb (2000) |
| $\theta_0$ | Water content at air-dry conditions | $0.03 \times \theta_{fc}$ | – | Assumed 3% WHC |
| $\nu_{POC}$ | Maximum specific decomposition rate of POC | $1.7 \times 10^{-5}$ | 1/min | Calibrated |
| $\mu_{AC}$ | Maximum specific uptake rate | $3.5 \times 10^{-4}$ | 1/min | Calibrated |
| $\mu_{CR}$ | Maximum specific mineralization rate by CR | $1.75 \times 10^{-4}$ | 1/min | Assumed equal to $\mu_{AC}/2$ |
| $\xi_c$ | Saturation coefficient of DOC | Michaelis-Menten eq. | – | Michaelis and Menten (1913) |
| $\xi_{EE}$ | Saturation coefficient of EE | Reverse Michaelis-Menten eq. | – | Wang and Post (2013) |
| $\pi_b$ | Microbial turgor pressure | 1022.7 | cm | Assumed constant (Manzoni et al., 2014) |

(*continued on next page*)

**Table 2** (*continued*)

| Parameter | Description | Value | Units | Notes and refs. |
|---|---|---|---|---|
| $\Pi_{os}$ | Switch factor for osmolyte production/elimination | Eq. (33) | – | |
| $\tau_i$ | Maximum specific inactivation rate | $2 \times 10^{-6}$ | 1/min | Calibrated |
| $\tau_{os}$ | Maximum specific rate of osmoregulation | $6 \times 10^{-4}$ | 1/min | Calibrated |
| $\tau_r$ | Maximum specific reactivation rate | $1.4 \times 10^{-6}$ | 1/min | Assumed equal to $\tau_i$/1.43 (Konopka, 2000) |
| $\chi_a$ | Coefficient of water-stress | Eq. (17) | – | Calibrated using respiration data before RW from Meisner et al. (2017) |
| $\chi_{os}^r$ | Coefficient of osmoregulation | Eq. (22) | – | |
| $\chi_{os}^s$ | Coefficient of osmotic stress | Eq. (21) | – | |
| $\chi_\tau$ | Coefficient of tortuosity | Eq. (16) | – | Hamamoto et al. (2010) |
| $\psi_{fc}$ | Water potential at the field capacity | 348 | cm | Richards and Weaver (1944) |
| $\psi_{M,os}$ | Maximum water potential compensated by osmoregulation | $-1.5 \times 10^5$ | cm | Water potential that restricts activity of most of species in e.g., Manzoni et al. (2012a) |
| $\psi_0$ | Water potential at air-dry conditions | $-1.5 \times 10^5$ | cm | Water potential at which microbial activity ceases (e.g., Manzoni and Katul, 2014) |
| $\psi^*$ | Water potential matching point in the modified Webb's equation | Eq. (15) | cm | Based on Webb (2000) |

severity of the conditions to which microorganisms have been exposed (Stolpovsky et al., 2011). This drought-legacy effect on reactivation rates is regulated through $\Gamma_m$. The respiration cost of dormancy (reactivation) is given by $z_r R^{DC}$. Inactive microorganisms reduce their exposure to adverse experiences, resulting in lower decay rates and no need for osmoregulation.

### 2.7. Mineralization by cell residues

The model also incorporates a mechanism to explain the contribution of extracellular compounds to soil respiration (as demonstrated by Fraser et al., 2016; Kéraval et al., 2016; Maire et al., 2013). Those cells that do not efficiently compensate osmotic stress (by osmoregulation or dormancy) might experience osmolysis and release their cytoplasm and intra-cellular compounds. A $\lambda_z$ fraction of these cells is assumed to remain in the system as extracellular compounds (here CR), which can still perform catabolic reactions, but they are not able to grow. In this way, CR compete with AC for DOC and contribute to respiration ($C^{CR}$).

### 2.8. Biomass growth, respiration, and CUE

Derived from the processes defined above, the equations for growth and respiration are written as,

$$\text{Growth} = \underbrace{y^* U^{AC}}_{\text{Biomass synthesis}} \tag{10}$$

$$\text{Respiration} = \underbrace{(1-y^*)U^{AC}}_{\text{Biomass synthesis costs}} + \underbrace{C^{CR}}_{\text{Mineralization by CR}} + \underbrace{(1-y_{os})E^{OS}}_{\text{Osmoregulation costs}} + \underbrace{z_r R^{DC}}_{\text{Dormancy costs}} \tag{11}$$

Growth is defined as the total amount of DOC that, after respiration, is invested in the synthesis of new microbial compounds, i.e., cells and enzymes. Respiration rates are the result of the costs associated with biomass synthesis, osmoregulation and dormancy, and the extracellular mineralization by cell residues. Note that the latter three processes are net contributors to respiration and do not add to growth, enhancing the decoupling between growth and respiration. Finally, the CUE value is defined as:

$$\text{CUE} = \frac{Growth}{Growth + Respiration} = \frac{\underbrace{y^* U^{AC}}_{\text{Biomass synthesis}}}{\underbrace{U^{AC}}_{\text{Uptake by AC}} + \underbrace{C^{CR}}_{\text{Mineralization by CR}} + \underbrace{(1-y_{os})E^{OS}}_{\text{Osmoregulation costs}} + \underbrace{z_r R^{DC}}_{\text{Dormancy costs}}} \tag{12}$$

## 3. Laboratory experiments and model comparison

We tested the ability of the presented model to reproduce the SOC dynamics induced by soil moisture changes, for i) wetting followed by drying and ii) wetting followed by stable soil moisture conditions (Fig. 1).

First of all, we calibrated the model by reproducing the respiration data presented in Miller et al. (2005), in which a soil was subjected to 4-week D/RW intervals during 16 weeks. This experiment has been widely used as a benchmark for models design to study the responses to D/RW. Respiration rates were estimated daily by measuring $CO_2$ production, while microbial growth rates were not measured. The microbial biomass was estimated at the beginning and end of the experiment. In our simulations, we reproduced the conditions to which the soil was exposed during the experiment itself, but also those from before (to incorporate drought-legacy effects). Dry soils were first stored 90 days at 4% WHC. When the experiment started, they were repeatedly rewetted to 60% WHC and let dry to air-dry conditions (as in Fig. 1, left-hand panels), mimicking the behavior of soils exposed to episodic rain. Second, we evaluated the capability of the model to reproduce the patterns for respiration and growth in soils exposed to a single cycle of D/RW where the moisture was kept constant after RW (Fig. 1, right-hand panels). This simulation allowed us to discuss the capability of the model to obtain pulses in respiration even when moisture did not recover its pre-RW value, and to unravel the actual mechanisms governing the response.

The model was manually calibrated using the respiration data from Miller et al. (2005), with the aim of capturing the observed behavior and assess which processes contribute to it. The calibration was thus meant to provide reasonable parameter estimates for theoretical explorations based on this particular case study, rather than to provide a parameter set for model validation. The parameter values were held within theoretically and physically realistic ranges (Table 2) and, when possible, based on Lawrence et al. (2009). POC was assumed at a pseudo steady-state in all simulations, assuming inputs equal outputs within the time frame studied. The system of equations was solved numerically

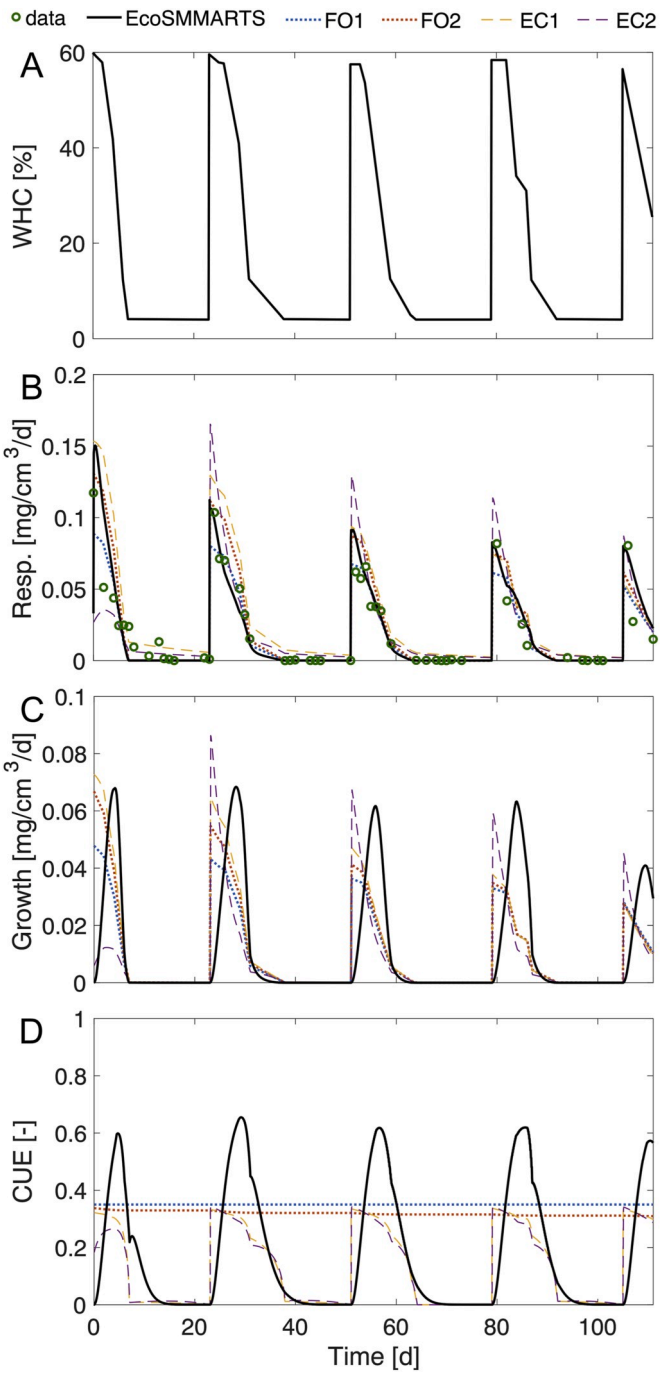


**Fig. 3.** Model simulations of the 4-week-interval D/RW experiment described in Miller et al. (2005). Comparison of the results obtained by the presented model (SMMARTS-Eco, solid black line) and LMs: FO1 (dotted blue), FO2 (dotted red), EC1 (dashed yellow), EC2 (dashed purple). Respiration measurements are indicated by green circle markers. Panels represent the dynamics of measured soil moisture (WHC [%], panel A), measured and modelled respiration rates ([mg/cm$^3$/d], panel B), growth rates ([mg/cm$^3$/d], panel C), and CUE ([-], panel D). (For interpretation of the references to colour in this figure legend, the reader is referred to the Web version of this article.)

using a fully explicit finite difference scheme. The time steps were decreased to the order of seconds upon RW, and recovered slowly to minutes, as perturbation effects vanished. The readjustment of time steps allowed capturing the fast dynamics while keeping the computational costs low.

For comparative purposes, the process-based SOC models in

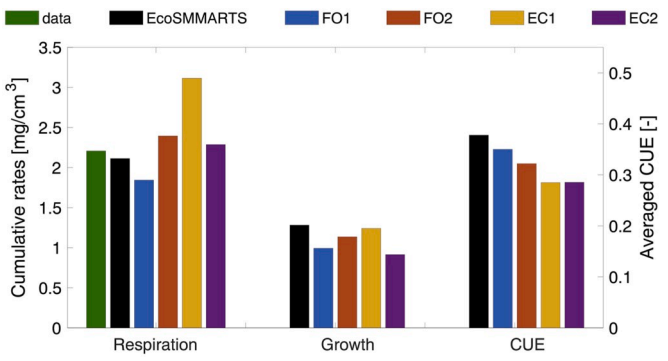


**Fig. 4.** The total amount of C lost as respiration [mg/cm$^3$], invested in growth [mg/cm$^3$] and the resulting CUE [-] over 111 days in the 4-week-interval D/RW experiment described in Miller et al. (2005). Comparison of the results obtained by the experimental data (green bars; only respiration measured), the presented model (SMMARTS-Eco, black bars) and LMs: FO1 (blue bars), FO2 (red bars), EC1 (yellow bars), EC2 (purple bars). (For interpretation of the references to colour in this figure legend, the reader is referred to the Web version of this article.)

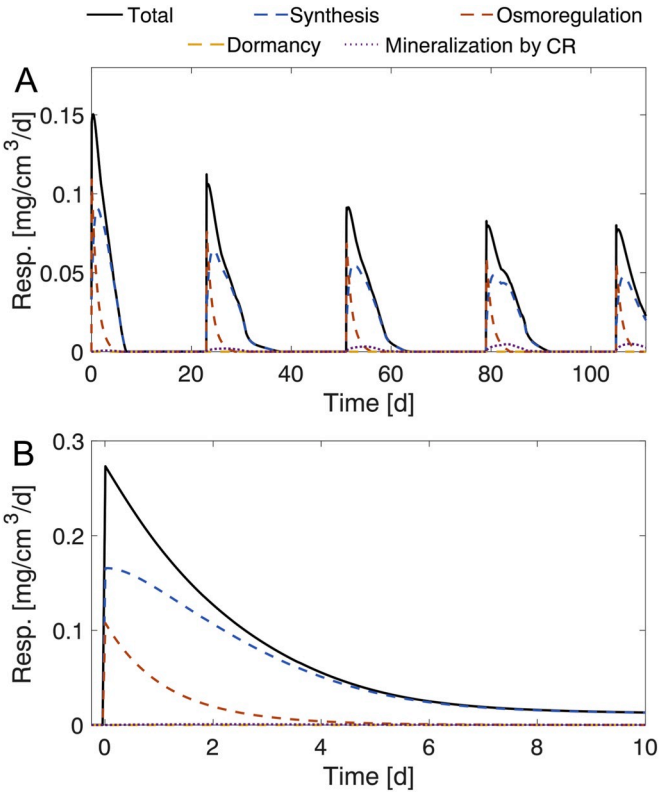


**Fig. 5.** Contributions of different processes to the total amount of C respired [mg/cm$^3$/d] (thin black lines) according to simulations by the EcoSMMARTS model parameterized for Miller's experiment (panel A; as in Fig. 3) or for the case of a single RW (panel B; as in Fig. 6). The processes included are synthesis of new biomass (in dashed blue), osmoregulation (dashed red), dormancy (dashed yellow), and mineralization by cell residues (dotted purple). (For interpretation of the references to colour in this figure legend, the reader is referred to the Web version of this article.)

Lawrence et al. (2009) were also included in this study. Lawrence and coworkers presented four different models (referred here as LMs) of increasing complexity that include a wide range of processes at soil-microbial level governed by soil moisture. The simplest model (FO1) assumes three C compartments representing the active, slow, and

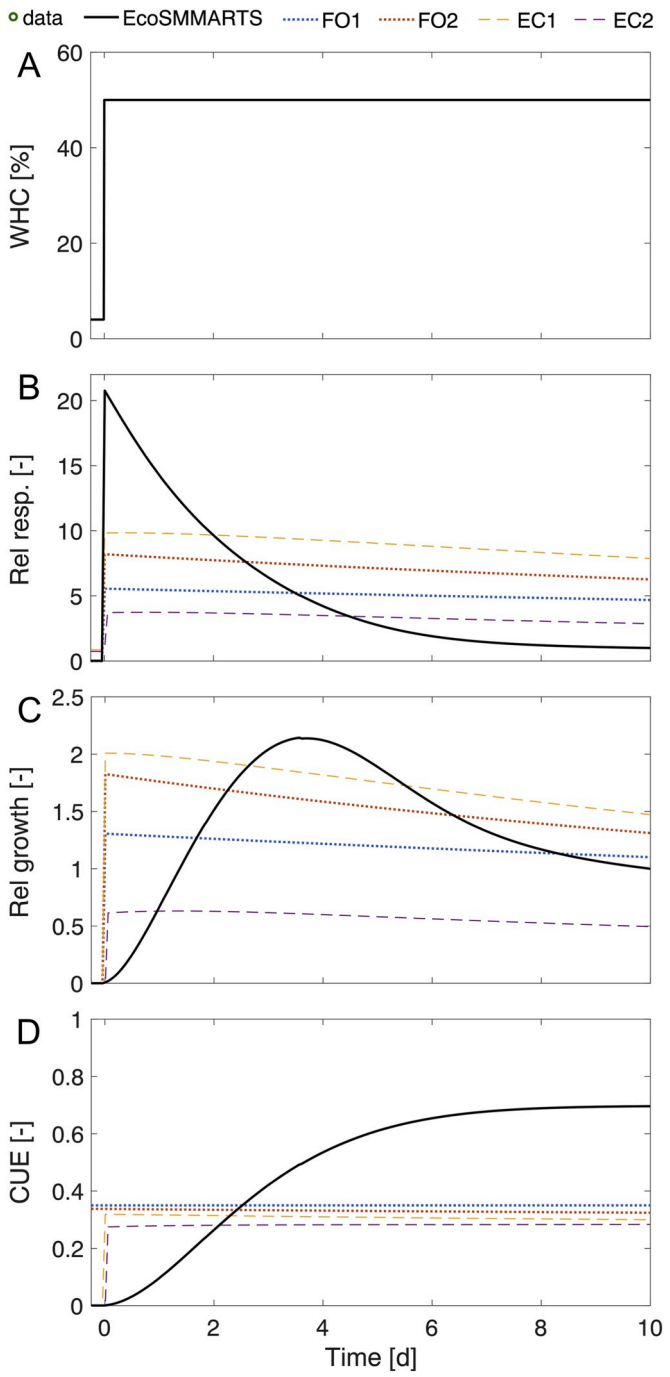


**Fig. 6.** Model simulations of the dynamic response of a 4% WHC air-dried soil that is rewet up to 50% WHC. Comparison of the results obtained by the presented model (EcoSMMARTS, solid black line) and LMs: FO1 (dotted blue), FO2 (dotted red), EC1 (dashed yellow), EC2 (dashed purple). The panels represent the 10-day dynamics of soil moisture (WHC [%], panel A), relative respiration rates ([-], panel B), relative growth rates ([-], panel C), and CUE ([-], panel D). Relative values are obtained by comparing the current rates to those obtained by the end of the EcoSMMARTS simulation (10 days after RW), when the effect of the disturbance has diminished. (For interpretation of the references to colour in this figure legend, the reader is referred to the Web version of this article.)

passive C pools, where microorganisms are considered part of the active pool. Microbial growth and respiration are defined as a fixed portion of the C that is decomposed from the two other pools. The FO2 model includes microbial maintenance expenses in the respiration rates and distinguishes between DOC and microbial compartments, while other features remain similar to FO1. The most complex models (EC1 and EC2) consist of a more detailed description of soil processes by incorporating additional C compartments and fluxes. The active pool in EC2 is subdivided in three pools: dissolved C (but unavailable), bio-available C, and microbial biomass; moreover, an enzyme pool acts as a catalyzer of decomposition. These models incorporate some supplementary processes that might influence SOC dynamics, such as the synthesis and payoff of enzymes, the potential accumulation of bio-available C, the partitioning of microbial turnover, and the interaction between C and soil particles by sorption-desorption reactions. The resulting growth rates in EC2 (most complex model) is similar to those in FO1 (the simplest) but here C is only sourced from the bio-available pool and the amount of microbial biomass is included as a rate modifier. Respiration then contains two terms associated with microbial growth and maintenance, but is also fed by a fraction of the C used for the synthesis of enzymes. In our simulations, LMs were re-implemented as accurately as possible based on the equations presented in Lawrence et al. (2009) to allow for comparisons with EcoSMMARTS (details in the MATLAB files linked).

## 4. Results

### 4.1. Decoupled respiration and growth during D/RW cycles

We first studied the simulated responses to a series of D/RW events with frequency intervals of 4 weeks (Fig. 3, panel A) from Miller et al. (2005). Both LMs and EcoSMMARTS model were able to capture the respiration rates measured in the laboratory (green circle markers, panel B in Fig. 3) and the cumulative emissions (green bars in Fig. 4). Respiration rates responded rapidly to soil moisture increases by exhibiting sudden emission peaks of similar magnitude, followed by sharp exponential decreases with soil drying. The EcoSMMARTS model estimated respiration peaks that ranged between 0.08 and 0.11 mg/cm$^3$/d upon RW (excluding the first peak that was strongly influenced by the initial conditions). Emission rates decreased significantly as moisture dropped to 4% WHC. There was a tendency for gradually smaller peaks after every RW, as also observed in Miller et al.'s data. The soil released approximately 72% of the $CO_2$ within the 4 days following each pulse, while only $<$0.05% of the C was emitted under air-dry conditions (corresponding to 13.4% of the time). The small differences in respiration dynamics among the different models caused relatively large differences in the long-term. By the end of the experiment, the total C respired by LMs' simulations were from 13% smaller to 47% larger than that by the EcoSMMARTS model (Fig. 4). A detailed analysis of the EcoSMMARTS results also showed an uneven contribution of the different processes to respiration (Fig. 5, panel B). The percentages of respiration associated with the synthesis of biomass, osmoregulation, dormancy and mineralization by cell residues were 75%, 21%, $<$1% and 4%; respectively.

The simulated growth rates showed more clearly the conceptual differences between models (Fig. 3, panel C). The patterns of growth by all LMs were virtually identical to those for respiration (dashed and dotted lines in panels B and C). In contrast, the EcoSMMARTS model captured the expected disconnection between respiration and growth (solid lines). With this model, the growth rates started increasing linearly after RW and peaks were only achieved after about 4 days after RW (albeit this delay strongly depended on the dynamics of moisture). Microbial biomass synthesis in the first 4 days after each RW event encompassed only 39% of the biomass synthesized over the whole experiment (compared to the 72% for respiration). In the long term, the cumulative growth obtained from LMs was from 3% to 29% lower than that from the EcoSMMARTS model (Fig. 4).

The simulated CUE (Fig. 3, panel D) varied through time in the more complex among LMs. Simulations by EcoSMMARTS resulted in even more variable CUE due to the further disconnection between respiration

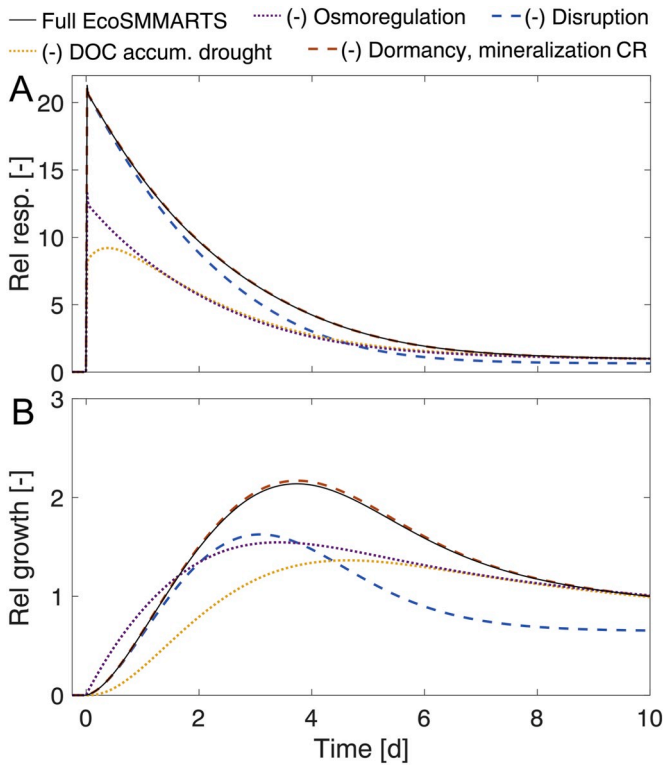


**Fig. 7.** Sensitivity analysis of processes in EcoSMMARTS, described trough: A) relative respiration rates [-], and B) relative growth rates [-] during a single D/RW event in which a soil initially air-dried at 4% WHC was rewet to 50% WHC. Each curve represents a simulation where one of the following processes was deactivated: osmoregulation (in dotted purple), DOC accumulation during drought (dotted yellow), aggregate disruption (dashed blue), and dormancy and mineralization by cell residues combined (dashed red). For reference, the results from the sensitivity analysis were compared to those from Fig. 6 (here: full EcoSMMARTS; solid thin black lines). The relative values were obtained by normalizing the rates to the value of the reference curve by the end of the simulation. (For interpretation of the references to colour in this figure legend, the reader is referred to the Web version of this article.)

and growth. The continued exposure to changing conditions during D/RW cycles kept the CUE in the EcoSMMARTS model away from the optimal conditions (CUE of biomass synthesis $= y^* = y = 0.7$; see Eq. (9)). Despite the differences in CUE among models (Fig. 3, panel D), the averaged CUE (calculated with the cumulative rates by the end of the simulations) were quite consistent (Fig. 4).

### 4.2. *Decoupled respiration and growth under steady soil moisture after a single rewetting*

The analysis of the patterns in soils exposed to RW in which soil moisture was then kept at the optimal level revealed the hidden dynamics behind a moisture disturbance. The different nature of the processes and mechanisms included in EcoSMMARTS and LMs yielded contrasting microbial responses to RW (Fig. 6). In LMs, both respiration and growth increased with increasing soil moisture and slowly decayed through time (<27% decrease in all rates 10 days after RW). Both rates remained relatively high as long as the soil moisture was kept close to the optimal conditions (note that we were far from depleting the substrate pools, which would have reduced C cycling rates). The EcoSMMARTS model reproduced disconnected patterns under the same conditions. On the one hand, respiration rates (solid black line in Fig. 6, panel B) peaked and decreased rapidly thereafter. The respiration peak was about 20 times larger than the respiration rate at the end of the simulation (presumably near to the steady state level). In this

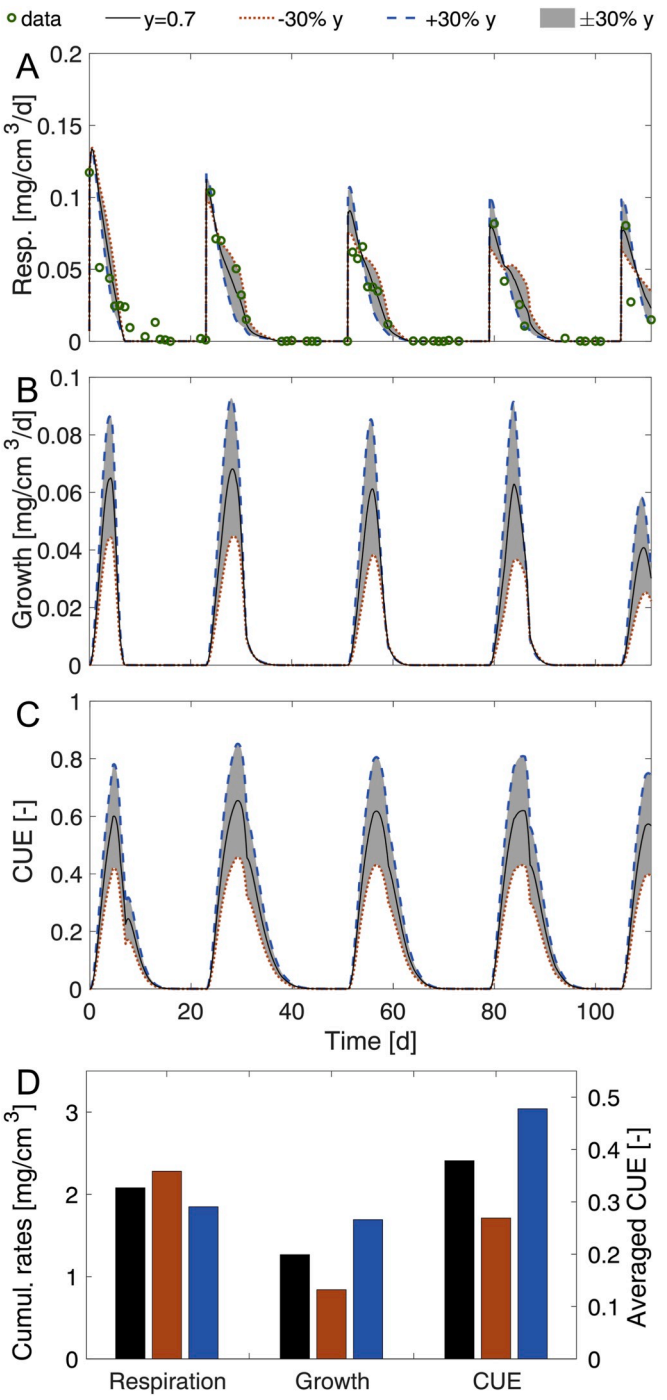


**Fig. 8.** Sensitivity analysis of the yield coefficient of C uptake ($y$) in the EcoSMMARTS model based on the Miller's experiment. The panels show the relative respiration rates ([-], panel A), relative growth rates ([-], panel B), CUE ([-], panel C) and the cumulative amount of C lost as respiration [mg/cm$^3$], invested in growth [mg/cm$^3$] and the resulting CUE [-] (panel D). For reference, the results from the sensitivity analysis were compared to those from Fig. 3 (black lines in B-D) and Fig. 4 (black bars). The simulations represented in red and blue are the results obtained by assuming a modification on $y$ by −30% and +30%, respectively. The grey shaded areas enclose the results obtained from the whole range ±30%. (For interpretation of the references to colour in this figure legend, the reader is referred to the Web version of this article.)

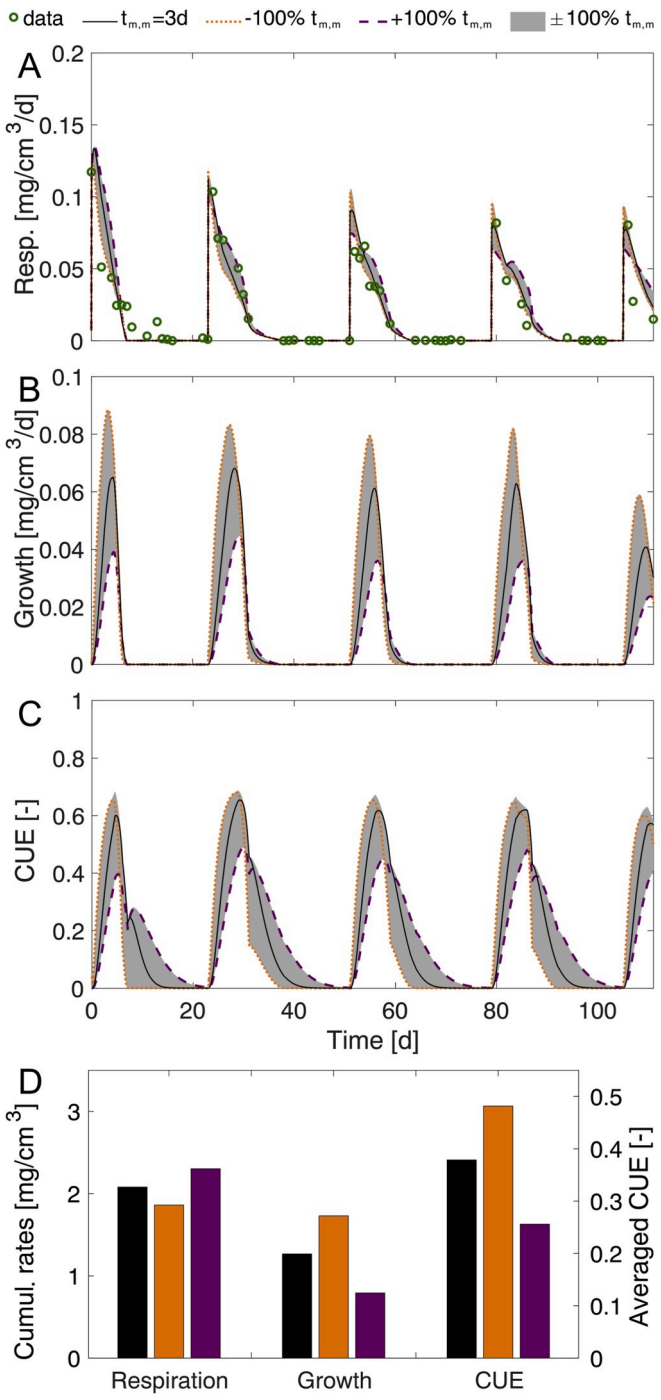


**Fig. 9.** Sensitivity analysis of the coefficient of memory ($t_{m,m}$) in the EcoSMMARTS model based on the Miller's experiment. The panels show the relative respiration rates ([-], panel A), relative growth rates ([-], panel B), CUE ([-], panel C) and the cumulative amount of C lost as respiration [mg/cm$^3$], invested in growth [mg/cm$^3$] and the resulting CUE [-] (panel D). For reference, the results from the sensitivity analysis were compared to those from Fig. 3 (black lines in B-D) and Fig. 4 (black bars). The simulations represented in orange and purple are the results obtained by assuming a modification on $t_{m,m}$ by −100% (no drought-legacy effect) and +100%, respectively. The grey shaded areas enclose the results obtained from the whole range ±100%. (For interpretation of the references to colour in this figure legend, the reader is referred to the Web version of this article.)

simulation, respiration was almost completely due to the synthesis of biomass and osmoregulation, which represented, respectively, 81% and 18% of the total amount of C respired (Fig. 5, panel B). On the other hand, growth rates followed different dynamics, characterized again by a slower response to RW (Fig. 6, panel C), a peak about 3.5 days after RW (reaching ≈2 times the steady-state), and a subsequent decrease. As a result, the CUE showed a smooth but slow recovery after RW, increasing as a sigmoidal function from almost 0 to an asymptotic value close to the CUE of biomass synthesis (CUE→$y$ = 0.7).

### 4.3. Sensitivity analysis

The importance of the different features in the EcoSMMARTS model in determining microbial dynamics was analyzed based on the response to a single D/RW event (Fig. 7). The processes studied were osmoregulation, initial DOC availability via its accumulation during drought, aggregate disruption, dormancy and mineralization by cell residues (from Sections 2.3-2.7). To do so, these processes were sequentially activated and deactivated. When a process was deactivated, the associated C fluxes were set to zero (i.e., neither production, nor transformation or decay), thus removing their contributions to respiration and growth. The influence by the DOC accumulation during drought was deactivated by setting the initial mass of DOC to zero. Therefore, in Fig. 7, curves close to the result of the full model (thin black curve) indicate that specific processes have little impact because even when they are removed, the model produces a nearly complete response.

Results from simulations showed that the shape of the response to RW was preserved even though some processes were inactive (Fig. 7; comparison between the thin black line and all others). Specifically, osmoregulation (dotted purple) and DOC accumulation during drought (dotted yellow) were the main mechanisms determining the amount of C fueling the respiration response, and controlled the size and abruptness of the peaks. Although the disruption of soil aggregates also contributed to C supply, its effects did not influence the first phase of the respiration response, but did instead alter its tail and the entire growth dynamics (dashed blue), which suggests its relevance in the long term. With this specific choice of parameters, the dormancy and mineralization by cell residues combined (dashed red) had no relevant effect on the respiration and growth dynamics (for a discussion, see Section 5.3.2.2).

Moreover, we targeted specific parameters important for the CUE (those determining growth rates through Eq. (9)) and conducted a sensitivity analysis on C uptake yield $y$ (±30%) and memory duration $t_{m,m}$ (±100%), using the 4-week-interval D/RW experiment from Miller et al. (2005). First, changing $y$ by ±30% had little effect on the respiration rates and did not alter the capability of the model to capture the empirical observations (Fig. 8). Microbial growth retained the shape but the magnitude of the peaks changed substantially, resulting in a 34% increase in the accumulated growth. Surprisingly, the scenario where more C is used for growth (+30%$y$) showed higher respiration peaks upon RW (dashed blue line compared to black and red, panel A in Fig. 8), even though the cumulative respiration was smaller (columns in panel D). A more efficient growth promoted larger active populations (not shown), which could transform and make use of larger amounts of DOC faster, causing higher peaks. The scenario with lower efficiencies (−30% $y$; in dotted red) resulted in smaller and smoother peaks for both growth and respiration. Similarly, the memory duration $t_{m,m}$ had a small influence on respiration but showed larger effects on growth and CUE (Fig. 9). When the legacy of drought was neglected (−100% $t_{m,m}$ = 0; in orange), the delay in growth was reduced but not completely eliminated. The reason is that the effects of osmotic stress on $y^*$ (Eq. (9)) were still inhibiting the synthesis of biomass, but the resilience capacity of the microbial community was notably higher and the efficiency was recovered rapidly after RW. In this way, DOC could be used for growth earlier, maintaining the growth and respiration patterns but shifting the whole response earlier. Larger drought-legacy effects on

microorganisms (memory duration +100% $t_{m,m}$ = 6d; in purple) resulted in a slower microbial growth after RW and a lengthening of the period of recovery. For the studied set of parameters, when the community was eventually able to grow efficiently ($y^* \rightarrow y$), the moisture conditions were no longer suitable, resulting in reduced C accumulation in biomass.

## 5. Discussion

### 5.1. Microbial respiration driven by soil moisture changes

After calibration, the respiration pulses simulated by the EcoSMMARTS model reproduced the dataset from Miller et al. (2005) well. These patterns in respiration had also been obtained before using other models (e.g., Evans et al., 2016; Lawrence et al., 2009; Li et al., 2010). All these models predict that RW of dry soils causes a peak in the $CO_2$ emissions followed by a rapid decrease, agreeing with the textbook definition of the "Birch effect" (Birch, 1958; Jarvis et al., 2007). Empirical studies have reported high variability in $CO_2$ emissions, in which respiration peaks increased from 2 to 45 times over those measured previous to the RW event in pulses that lasted from a few hours to several weeks (see review by Kim et al., 2012). In line with these empirical observations, the size and duration of respiration pulses obtained by the EcoSMMARTS model varied significantly across simulation scenarios, because they were dependent on the properties of the RW event (moisture change, velocity of RW, duration of moist conditions, drying curve …), but also those of the dry period preceding it (duration, severity …). In general, we found more intense respiration peaks in soils exposed to lower frequencies of RW (as in Fierer and Schimel, 2002; Miller et al., 2005; Wu and Brookes, 2005) and to more long and intense drought (as in Barnard et al., 2015; Fischer, 2009; Kieft et al., 1987; Lado-Monserrat et al., 2014). The results also revealed that about three-quarter of the C emissions were generated during the 4 initial days after each RW event, and that the contribution under completely air-dry conditions was low. Therefore, models consistently recognize the responses to D/RW as strong contributors to the cumulative $CO_2$ emissions and the long-term C stocks.

We also found that the short-term dynamics could lead to misleading expectations in the long term. For instance, when we assumed high microbial growth efficiency (+30% $y$; dashed blue line in panel A, Fig. 8), the respiration peaks immediately after RW were higher than those in the 'control' model runs. Despite this, the cumulative respiration after several D/RW cycles was lower (blue bar in panel D). A detailed analysis of the results revealed that continuous larger investments in growth led to a larger microbial community, which was able to respire more and faster when the next RW event occurred, but also to grow and deplete the C resources faster, which is analogous to previously documented patterns (de Nijs et al., 2018). This cascade of events pointed out the importance of studying D/RW at the appropriate temporal scales – if the goal is to assess consequences for C stocks, several D/RW cycles at high temporal resolution should be considered to account for long-term effects caused by the nonlinear processes taking place.

That microbial respiration would decrease with drier conditions is not surprising, and can easily be explained by a direct dependence of microbial activity on the soil moisture level. Under stable steady state conditions in soils, such moisture dependencies are reasonably well known (Manzoni et al., 2012a), and represent information that has already been incorporated into process-based models and even Earth System Models (e.g., Bauer et al., 2008; Sierra et al., 2015). To determine if a respiration pulse is induced by RW, the most common approach is therefore to maintain stable moisture after RW (e.g., Chase and Gray, 1957; Chowdhury et al., 2011; de Nijs et al., 2018; De Nobili et al., 2006; Griffiths and Birch, 1961; Kieft et al., 1987; Meisner et al., 2013; Placella et al., 2012; Wu et al., 1997), and thereby exclude the influence of the direct effect by soil moisture. When moisture was maintained following RW (Fig. 1, right-hand panels), responses simulated using the set of parameters used in LMs (Fig. 6) generated no respiration peaks. As such, all versions of LMs failed to capture the respiration pulse induced by RW dry soils, beyond the direct effect of soil moisture. In contrast, the EcoSMMARTS captured large pulses of respiration even in soils that were kept at constant moisture after RW (in line with empirical observations in, e.g., de Nijs et al., 2018; Fierer and Schimel, 2003; Griffiths and Birch, 1961; Kieft et al., 1987; Meisner et al., 2013; Placella et al., 2012; Wu and Brookes, 2005; Yu et al., 2014). Therefore, the RW and the cascading effects it triggers were revealed as the drivers of $CO_2$ emissions. The pre-RW respiration rates were not restored after RW since the new conditions (optimal moisture) resulted in a new steady state. The soil moisture level after RW determined the base-line respiration (once the effect of the perturbation had vanished). All this suggested that the daily average moisture content used in many biogeochemical models (e.g., Allison and Goulden, 2017; Lawrence et al., 2009; Li et al., 2010; Smith et al., 2014) could be inadequate to capture the influence of D/RW on C dynamics, calling for including both the fluctuations of moisture and the cascading effects they trigger at a higher temporal resolution.

### 5.2. Microbial growth and the resulting CUE driven by soil moisture changes

The EcoSMMARTS model effectively captured patterns of biomass synthesis and CUE reported in the literature (e.g., Blazewicz et al., 2014; Iovieno and Bååth, 2008; Meisner et al., 2013). In contrast to the rapid increase in respiration, the growth rates started increasing slowly in a linear fashion after RW, achieving maximum productivities a few days after the respiration peak, and then decreased (Figs. 3 and 6). This decoupling between respiration and growth was particularly significant during the first stages after RW. Besides the processes contributing to respiration and not to growth (Section 5.3), soil microorganisms went through a transition period of low growth compared to C uptake, and thus low CUE. Despite the apparent abundance of resources (as shown by the respiration pulse), C did not equivalently contribute to growth (see Section 5.3). The velocity at which CUE was restored after RW depended on the resilience of the community to withstand the drought-legacy effects (e.g., Fig. 9), which could arise from a combination of microbial physiology responses, trait changes within populations and species sorting (Chapin et al., 2002; Manzoni et al., 2012b; Schimel et al., 2007). In general, those microorganisms exposed to shorter and less intense periods of drought could invest larger amounts of resources to growth. Yet, the strong influence of the drought-legacy effects on the long-term C stocks (as shown in e.g., Figs. 8 and 9) suggested that scenarios with contrasting responses to D/RW frequency could be also possible (as in Fierer and Schimel, 2002; Shi and Marschner, 2014).

In contrast with the EcoSMMARTS model, the microbial growth patterns in Figs. 3 and 6 could not be captured by current models (represented here by LMs but also valid for Evans et al., 2016; Li et al., 2010; Manzoni et al., 2014, and others), which overlooked growth and did not include the mechanisms to induce a sufficient decoupling between respiration and growth. In general, both rates were assumed to be a constant fraction of the C taken up, resulting in a strong synchronization of their patterns and small differences in CUE (albeit notable during dry periods when C uptake was very low and other processes became important, such as maintenance respiration).

Surprisingly, the LMs resulted in very little differences in the longer-term cumulative growth compared to the EcoSMMARTS (Fig. 4), but rather a redistribution of growth and respiration over time. However, the mismatch of LMs simulation of microbial growth compared to new empirical observations (discussed above) might imply a misinterpretation of the mechanisms governing C sequestration during D/RW.

### 5.3. Which mechanisms need to be invoked to capture respiration and growth dynamics?

The calibration of the model permitted to capture the observed behavior and assess which processes contributed the most to C fluxes in this particular case study. It can be argued that a model of this complexity is likely to fit any data set thanks to the large number of parameters, but it could also capture the observed patterns for wrong reasons. Indeed, even simpler models have been shown to have both equifinality issues and weak compartment structures (Marschmann et al., 2019). The EcoSMMARTS model, however, was developed for theoretical exploration rather than prediction, based on processes and mechanisms described in the literature and using plausible parameter values. With this background in mind, in this section we interpret model results to identify key processes driving microbial responses to D/RW.

#### 5.3.1. DOC accumulation during drought

Under dry conditions, both respiration and growth rates were strongly inhibited. Yet, the number of soil processes still ongoing progressively set the conditions that influenced the subsequent response upon RW. Despite the limited POC decomposition under low moisture conditions, simulations showed a ubiquitous accumulation of DOC during dry events (in agreement with Homyak et al., 2018; Miller et al., 2005; Schaeffer et al., 2017), which fueled the response to RW. Even though similar results were obtained in models by Evans et al. (2016) and Manzoni et al. (2014) via physiological and diffusion limitations on C accessibility, they lacked the structure necessary to describe decoupled growth and respiration at RW.

The increased DOC availability upon RW in our simulations was promoted by a combined effect of a reduced microbial activity accompanied by a low (but larger than microbial uptake) transformation of different forms of C to DOC. On the one hand, microbial activity and C uptake were low during dry periods due to the limited microbial access to substrates (e.g., Manzoni et al., 2016; Yarwood et al., 2006) without the need to define environments spatially separated (as in Evans et al., 2016). On the other hand, DOC was continuously sourced from recycled products of decay and from POC decomposition (via exoenzymatic activity), which could still take place in microscale soil patches inaccessible for microorganisms (Schimel and Schaeffer, 2012; Vetter et al., 1998; Wu and Brookes, 2005). Additionally, soils exposed to severe drought resulted in larger C availabilities after RW due to the physical disruption of soil aggregates, which exposed previously protected SOC to decomposition (Fierer and Schimel, 2003; Homyak et al., 2018; Navarro-García et al., 2012). The duration and intensity of the dry period preceding RW determined the amount of DOC accumulated, which resulted in larger respiration pulses when the intervals between RW events were longer (as in Fierer and Schimel, 2002; Miller et al., 2005). The duration of the dry period also defined the physiology of the community (e.g., the number of active and surviving organisms, the amount of osmolytes, the stress-level of cells), which determined their resilience and the patterns of the responses when conditions improved upon RW.

#### 5.3.2. The microbial mechanisms that induced decoupled dynamics during D/RW

The result that an important part of the C available upon RW was not used for growing purposes, but respired, implied the existence of mechanisms that decoupled growth from respiration. The low CUE characterizing the periods of low moisture endured several days after RW, suggesting drought-legacy effects on the response. To describe the differing contributions to respiration and growth rates, EcoSMMARTS assumed that resources were not used in the same way as, for instance, under optimal conditions, but the microbial communities activated strategies to mitigate the effects of stress and maximize survival (Brangarí et al., 2018; Tiemann and Billings, 2011), at the cost of lower CUE.

##### 5.3.2.1. Synthesis of biomass.

We identified the synthesis of biomass as a mechanism that governs the decoupling. Of the DOC taken up by microbial communities, only a fraction is used for growth and the rest is lost through respiration. In the model, this fraction changes over time due to the legacy effect of the previous dry period on the synthesis of new biomass (via the effective yield coefficient of C uptake $y^*$; Eq. (9)). The CUE of biomass synthesis was very low upon RW but then gradually recovered as the microbial community adapted to the new conditions, inducing a delay in microbial growth rates. When communities were exposed to extended dry periods, C was not efficiently used for growth since water and C limitation restricted the physiological adaptation (Schimel, 2018; Tiemann and Billings, 2011). After RW, despite the apparent abundance of resources, the microbial community was still burdened by osmotic stress and the drought-legacy effects on growth efficiency. This legacy effect can be attributed to the increased cell repair and maintenance costs required to resume growth (Amato et al., 2010; Sun et al., 2017). As a result, the CUE of biomass synthesis was very low upon RW but then gradually recovered, inducing a delay in microbial growth rates, as the microbial community adapted to the new conditions.

##### 5.3.2.2. Osmoregulation.

Even though osmolytes have been reported only in some soils (e.g., Boot et al., 2013; Kakumanu et al., 2013; Warren, 2016), our simulations suggest that osmoregulation contributed substantially to the decoupling of growth and respiration. To compensate water potential stress, large amounts of intracellular osmolytes were synthesized during dry periods, and were subsequently eliminated after RW. This osmoregulation process had significant implications for the CUE. First, the simple efflux of compounds contributed significantly to the initial respiration peak (Fig. 5). According to Sleator and Hill (2002) and Wood et al. (2001), a significant fraction of the osmolyte-C could be used to activate mechanisms that mediated their efflux, such as the activation of channels in cell membranes. Second, the released osmolytes remained close to cells (here as DOC) and could be re-assimilated afterwards (Slessarev et al., 2020; Williams and Xia, 2009), promoting delayed growth. Such a rapid reuse of osmolytes was in line with the difficulties on measuring osmolytes in their extracellular form (Boot et al., 2013; Göransson et al., 2013). Third, the osmotic-stressed communities exhibited lower efficiencies in biomass synthesis (Section 5.3.2.1).

##### 5.3.2.3. Other potentially significant mechanisms.

In the simulations presented here, both dormancy and mineralization by cell residues had very small contributions to the overall dynamics, suggesting that they could have been omitted from the model. However, there is empirical evidence to believe that these two features should be represented in EcoSMMARTS, because they can play more important roles in the longer term or under other scenarios, where the response to RW have even depicted categorically different patterns (e.g., Göransson et al., 2013; Meisner et al., 2013; or Xiang et al., 2008).

First, previous models showed the importance of dormancy on microbial and soil C dynamics (Brangarí et al., 2018; Manzoni et al., 2014; Placella et al., 2012; Salazar et al., 2018). Although this mechanism resulted in a low contribution in the simulations presented here, the resulting dynamics were in line with empirical observations (too small to discern in Fig. 5). In particular, the respiration costs associated with cellular reactivation from dormancy were small but consistent after RW. Additionally, the process of reactivation did not contribute to growth, but the reactivated cells were incorporated in the AC pool, competing for resources and thus delaying the overall growth response.

Second, respiration has been measured in soils deprived of all observable cellular forms (such as soils sterilized by γ-irradiation or chloroform fumigation) and its isotope fractionation was incompatible with respiration of cellular origin (Fraser et al., 2016; Kéraval et al., 2018, 2016; Maire et al., 2013). In line with their observations, our

model proposes that those cells that did not properly compensate the effects of water stress by osmoregulation or dormancy experienced cell lysis. The residues released from dead organisms could remain in the system without performing anabolic processes, but they could still carry out biogeochemical reactions of catabolism, contributing to respiration peaks and reducing the amount of DOC allocated to growth. However, the contribution of this mechanism was small and not necessary to explain the dynamics discussed in this paper.

### 5.4. Implications at bigger scales

The study of these microbial and biogeochemical mechanisms during D/RW is necessary to predict the future soil C stocks since the short-term dynamics under study can contribute more significantly to the large-scale and long-term ecosystem's functioning than other gradual changes in climatic conditions. The outcomes of this study represent a step towards unravelling microbial responses to D/RW cycles (i.e., to drought and rainfall events), which can help disentangling the role of soils in the global C cycle (and C sequestration) and their future importance under scenarios of climate change. Despite the promising advances in the field, additional research is required to evaluate the influence of these dynamics at the large scale and on the long term, combining empirical and modeling approaches across scales.

## 6. Conclusions

The EcoSMMARTS model was able to capture the respiration peaks in soils exposed to repeated cycles of D/RW and, unlike previous models, also to single RW events followed by constant moisture. In addition to this, the model reproduced the delayed microbial growth and the subsequent dynamic CUE, which were only recently uncovered experimentally and neglected in previous models. The fluctuating dynamics discussed in this paper involve relatively large respiration pulses and long-lasting microbial acclimation or adaptation responses, which are modulated not only by the characteristics of the dry and rewetting events, but also by the succeeding moist period. The model results identify the C accumulation during dry periods, the drought-legacy effects on the synthesis of new biomass, and osmoregulation as the strongest candidate mechanisms to explain C fluxes during D/RW. These three mechanisms provided both the C supply necessary to fuel the overall response and the timing necessary to reproduce the decoupled dynamics between respiration and growth.

## Declaration of competing interest

The authors declare that they have no known competing financial interests or personal relationships that could have appeared to influence the work reported in this paper.

## Acknowledgements

This work was supported by grants from Knut and Alice Wallenberg Foundation (KAW 2017.171), Swedish Research Council Vetenskapsrådet [grants 2015-04942, 2016-04146, 2016-06327] and Formas [grants 2015-468, 2018-01315, 2018-00425]. This research is a contribution to the strategic research area Biodiversity and Ecosystem services in a Changing Climate (BECC) at Lund University.

## Appendix 1. Soil moisture – soil water potential relation

The model requires the definition of a relationship between volumetric water content ($\theta_w$) and water potential ($\psi$), known as the water retention curve (WRC). As a starting point we selected the van Genuchten's curve (van Genuchten, 1980), which has been proven successful in capturing the WRC behavior for a wide variety of soils:

$$\theta_{vgn}(\psi) = (\theta_s - \theta_r)[1 + (\alpha|\psi|)^n]^{\frac{1}{n}-1} + \theta_r \tag{13}$$

where $\theta_s$ and $\theta_r$ are the saturated and the residual water contents, $n$ and $\alpha$ are two empirical coefficients that describe the type of soil and its pore structure, and $\psi$ is expressed in cm (1 KPa ≈10.197 $cmH_20$). However, Eq. (13) cannot reproduce properly the behavior of soils drier than the wilting point. The incorporation of a modified version of the Webb's log-linear expression (Webb, 2000) to the dry-end of the model ensures a smooth transition between the moist (from Eq. (13)) and dry (newly defined) regions by imposing a continuous first derivative in the matching point (see Schneider and Goss, 2012; Webb, 2000, for details). The resulting WRC is written as,

$$\theta_w(\psi) = \begin{cases} \theta_{vgn}(\psi), & \text{if } \psi \geq \psi^* \\ \gamma(\psi^*)[\log(|\psi|) - \log(|\psi_0|)] + \theta_0, & \text{if } \psi < \psi^* \end{cases} \tag{14}$$

where $\psi_0$ and $\theta_0$ are the water potential and the water content at air-dry conditions, respectively; and $\gamma$ is the derivative of the van Genuchten's curve in the semi-log scale. The coordinates of the matching point $(\psi^*, \theta_w^*)$ at which the derivative is evaluated can be found by solving iteratively the equation:

$$\frac{\theta_w^* - \theta_0}{\log(|\psi^*|) - \log(|\psi_0|)} = \ln(10)\psi^* \frac{d\theta_{vgn}(\psi^*)}{d\psi} \tag{15}$$

Most measurements of soil water content in empirical studies are expressed in terms of water holding capacity (WHC), which is the water content relative to the amount of water held by the soil after drainage (at 100% WHC). This value is also known as the field capacity ($\theta_{fc}$) and can be estimated as the moisture at a water potential $\psi_{fc} = -348$ cm (Richards and Weaver, 1944), solving Eq. (14).

## Appendix 2. Modeling the effect of soil moisture on C fluxes

In the EcoSMMARTS model, the influence of soil moisture on the intensity and occurrence of processes is regulated by means of the coefficients of tortuosity ($\chi_\tau$), water-stress ($\chi_a$), osmoregulation ($\chi_{os}^r$), osmotic stress ($\chi_{os}^s$), and drought-legacy effect on soils ($\Gamma_s$) or on microorganisms ($\Gamma_m$).

Based on the relationship between soil diffusivity and electrical conductivity under variably saturated conditions (in e.g., Archie, 1942; Hamamoto et al., 2010), $\chi_\tau$ can be written as

$$\chi_\tau(\theta_w) = \left(\frac{\theta_w}{\theta_s}\right)^{\gamma_\tau} \tag{16}$$

where $\theta_w$ is the volumetric water content of soil (see Appendix 1), and $\gamma_\tau$ is the shape parameter that determines the nonlinearity of this relationship. High values are achieved at saturated conditions, being $\chi_\tau = 1$ when $\theta_w = \theta_s$, and decreases as water films (the media where enzymatic activity takes place) shrink, becoming narrower and more tortuous.

The coefficient of water-stress $\chi_a$ describes the influence of moisture on substrate resources (limiting diffusivity) and the physiological stress experienced by microorganisms. It is defined as a lognormal expression, with mode $0.5\theta_{fc}$ (maximum at 50% WHC) and standard deviation equal 1 (matching the empirical observations before RW in Meisner et al., 2017).

$$\chi_a(\theta_w) = \frac{1}{\theta_w - \theta_0} exp\left(\frac{2ln(\theta_w - \theta_0) - \left[\ln\left(\frac{\theta_w - \theta_0}{0.5\theta_{fc} - \theta_0}\right)\right]^2}{2}\right) \tag{17}$$

The memory function defined in $\Gamma$ represents the drought-legacy effects on the soil-microbial system and can be defined as,

$$\Gamma(\theta_w) = \frac{\int_{-\infty}^{t} g(\tilde{\tau})\chi_a^* d\tilde{\tau}}{\int_{-\infty}^{t} g(\tilde{\tau}) d\tilde{\tau}} \tag{18}$$

where $g(\tilde{\tau})$ is the Gaussian kernel $g(\tilde{\tau}) = exp(-\tilde{\tau}^2/2t_m^2)$, being $t_m$ the standard deviation of the curve or the memory duration ($t_{m,s}$ for soils and $t_{m,m}$ for microorganisms), $\tilde{\tau}$ the time variable of integration, and

$$\chi_a^* = \begin{cases} \chi_a, & if\ \theta_w \le 0.5\theta_{fc} \\ 1, & if\ \theta_w > 0.5\theta_{fc} \end{cases} \tag{19}$$

The kernel shape is defined so that the more recent events have a stronger impact on $\Gamma$ (i.e., microorganisms have better 'short-term memory' than 'long-term memory'), but about 1/3 of the $\Gamma$ value comes from the conditions to which soils were exposed before the defined $t_m$. Note that $\Gamma$ is an indicator of the average severity of the dry events (where low $\Gamma$ suggest the recent experience of harsh conditions), but does not provide detailed information on the magnitude and frequency of the disturbances to which soils have been exposed.

Cells are also affected by osmotic stress or how strong the pressure gradient through cell membranes is. The optimal concentration of osmolytes in cells ($OS_{eq}$) changes with water potential. The drier is the soil the larger is the concentration of osmolytes required to maintain the turgor pressure $\pi_b$. $OS_{eq}$ can be estimated from the Van't Hoff relation (see Manzoni et al., 2014 for details) as,

$$OS_{eq}(\psi) = d_1 d_2 \frac{|\psi| + \pi_b}{RT} \tag{20}$$

where $d_1$ is a unit conversion coefficient, $d_2$ is the molecular weight of a representative osmolyte, $R$ is the gas constant value, and $T$ is the temperature in degree Kelvin. Based on this equilibrium, the indicator of the osmotic stress resulting from pressure imbalance can be written as,

$$\chi_{os}^s(\psi) = \frac{\left|OS_{eq}(\psi) - \overline{OS_{AC}}\right|}{OS_{eq}^{max}} \tag{21}$$

where $OS_{eq}^{max} = OS_{eq}(\psi_{M,os})$ in Eq. (20), being $\psi_{M,os}$ the lower water potential that can be compensated through osmoregulation. The higher is the osmotic stress, the larger is the mortality of AC; e.g., under osmotic shock at rewetting when excessive osmolytes cause cell lysis. The amount of resources required to survive under lower soil water potentials than $\psi_{M,os}$ are considered excessive and therefore, microorganisms in such dry soils can only use other survival mechanisms (e.g., dormancy).

The coefficient of osmoregulation $\chi_{os}^r$ regulates the production and the elimination of osmolytes in order to meet the equilibrium described above, as

$$\chi_{os}^r(\psi) = OS_{eq}^*(\psi) - \overline{OS_{AC}} \tag{22}$$

This indicator stands for the difference between the current osmolyte concentration ($\overline{OS_{AC}}$) and the intended one, which, based on Eq. (20) and $OS_{eq}^{max}$, can be defined as

$$OS_{eq}^* = min\left(OS_{eq}(\psi), OS_{eq}^{max}\right) \tag{23}$$

Finally, the combination of precipitation and evaporation during D/RW cycles results also in processes of dilution and evapo-concentration ($S^{DOC}$ and $S^{EE}$ in Eq. (2) and Eq. (6)), implying direct adjustments of $\overline{DOC}$ and $\overline{EE}$. These compounds experience a dilution upon RW and an increase in their concentrations during drying periods, both proportional to the change in the volumetric water content.

## Appendix 3. Detailed description of C fluxes and mass balance equations

In this appendix, the fully-parametrized form of the equations of the model EcoSMMARTS is presented. The model is essentially build on the previous work in Brangarí et al. (2018). The original SMMARTS model is adapted for ecological aspects by including a wide range of additional ecological insights, processes, compartments, and linkages to soil moisture. These new features come along with an increased complexity of the mechanisms leading the response to D/RW, which emphasize the disconnected contribution of processes into growth and respiration. SOC compounds are separated into eight lumped compartments: particulate organic carbon (POC), dissolved organic carbon (DOC), active cells (AC), dormant cells

(DC), extracellular enzymes (EE), osmolytes in AC ($OS_{AC}$), intracellular osmolytes in DC ($OS_{DC}$), and cell residues (CR).

The POC decomposition (into DOC) is a result of microbial foraging by enzymes and determines the amount of C that will be potentially available to microorganisms:

$$D^{POC} = \underbrace{[1 + m_d(1 - \Gamma_s)]\nu_{POC}\chi_t\xi_{EE}\overline{POC}}_{POC\ \ decomposition} \tag{24}$$

where $\nu_{POC}$ is the specific decomposition rate of POC, $\chi_t$ and $\Gamma_s$ are two coefficients denoting the effect of moisture on the processes (see Appendix 2 for details), $m_d$ is the coefficient of aggregate disruption, $\xi_{EE}$ is a saturating function of enzyme concentration formally equivalent to a reverse Michaelis-Menten expression (Wang and Post, 2013): $\xi_{EE} = \overline{EE}/(\overline{EE} + EE_k)$, in which $EE_k$ is the half-saturation constant of EE. The decomposition rates can be increased by aggregate disruption in those soils that experienced drought by a factor $[1 + m_d(1 - \Gamma_s)]$, where the value of $\Gamma_s$ decreases with the severity and duration of dry conditions experienced.

DOC uptake rates result from the competition between C availability (through $\xi_c$) and the potential microbial activity (denoted by the product $\chi_a\overline{AC}$),

$$U^{AC} = \underbrace{\mu_{AC}\chi_a\xi_c\overline{AC}}_{Uptake\ by\ AC} \tag{25}$$

where $\mu_{AC}$ is the maximum specific uptake rates, $\chi_a$ is the coefficient of water-stress (Eq. (17), Appendix 2), and $\xi_c$ is a saturation coefficient of DOC obtained from using a Michaelis-Menten expression with the half-saturation constant $DOC_k$. Only the fraction $y^*$ of $U^{AC}$ is effectively used for microbial growth (i.e., AC and EE), and not lost via respiration. $y^*$ varies with osmotic stress and drought-legacy effects (Eq. (9)). The fraction of C used to synthesize new EE is defined as,

$$\lambda^* = \lambda_{EE}(1 - \xi_{EE}) \tag{26}$$

Microorganisms can also switch between dormancy and activity through the sub-processes of inactivation ($I^{AC}$) and reactivation ($R^{DC}$), which depend on both C and water availability as follows:

$$I^{AC} = \underbrace{\tau_i(1 - \chi_a\xi_c)\overline{AC}}_{Inactivation} \tag{27}$$

$$R^{DC} = \underbrace{\tau_r\Gamma_m\xi_c\overline{DC}}_{Reactivation} \tag{28}$$

where $\tau_i$ and $\tau_r$ are the maximum specific rates of cell inactivation and reactivation, respectively; and $\Gamma_m$ is the coefficient of drought-legacy on microorganisms. Inactivation rates depend only on the current environmental conditions, while the legacy of drought determines their reactivation capacity (e.g., as in Stolpovsky et al., 2011). The energy required during dormancy contributes to respiration and is defined as $z_r$ times the reactivation rates.

During osmoregulation, osmolytes are produced ($P^{OS}$) or eliminated ($E^{OS}$) as

$$P^{OS} = \underbrace{(1 - \Pi_{os})\tau_{os}w_b\overline{AC}\chi_{os}^r}_{OS\ production} \tag{29}$$

$$E^{OS} = \underbrace{-\Pi_{os}\tau_{os}w_b\overline{AC}\chi_{os}^r}_{OS\ elimination} \tag{30}$$

where $\tau_{os}$ is the maximum specific rate of osmoregulation, $\chi_{os}^r$ is the coefficient of osmoregulation (Eq. (22); Appendix 2), $w_b$ is the cell-density conversion coefficient between volume of water in cells and dry mass of these cells, resulting in

$$\theta_{AC} = w_b\overline{AC} \tag{31}$$

$$\theta_{DC} = w_b\overline{DC} \tag{32}$$

and $\Pi_{os}$ is the switch factor activating either the production or the elimination of osmolytes depending on whether $\overline{OS_{AC}}$ is larger or smaller than the targeted concentration:

$$\Pi_{os} = \begin{cases} 1, & if\ \overline{OS_{AC}} \geq OS_{eq}^* \\ 0, & if\ \overline{OS_{AC}} < OS_{eq}^* \end{cases} \tag{33}$$

A fraction $y_{os}$ of the osmolytes that are expelled from cells (eliminated) are recycled into the DOC pool, while the rest is used as a source of energy during OS release through cell membranes.

Decay rates can be either associated to normal turnover (i.e., maintenance and ageing) or induced by stress. A fraction of such decayed products is recycled into DOC or POC. The normal turnover decay of each microbial compartment is defined similarly:

$$K^{AC} = \underbrace{k^{AC}\overline{AC}}_{AC\ natural\ decay} \tag{34}$$

$$K^{DC} = \underbrace{k^{DC}\overline{DC}}_{DC\ decay} \tag{35}$$

$$K^{CR} = \underbrace{k^{CR}\chi_a\overline{CR}}_{CR\ decay} \tag{36}$$

$$K^{EE} = \underbrace{k^{EE}\theta_w\overline{EE}}_{EE\ decay} \tag{37}$$

where $k^{AC}$, $k^{DC}$, $k^{CR}$, and $k^{EE}$ are the rate constants of decay for AC, DC, CR, and EE, respectively. Note that the decay of CR is additionally mediated by $\chi_a$, denoting the relatively fast recession of extracellular mineralization when conditions are restored (e.g., Meisner et al., 2017). Moreover, decay rates of cells can be largely accelerated under osmotic stress. Such an effect is included through

$$K_s^{AC} = \underbrace{k_{AC}^s\chi_{os}^s\overline{AC}}_{AC\ decay\ by\ stress} \tag{38}$$

where $k_s^{AC}$ is the rate constant for the stress-decay process and $\chi_{os}^s$ is the coefficient of osmoregulation (Eq. (21), Appendix 2). The decay rates for AC are assumed to be independent, so both $K_s^{AC}$ and $K^{AC}$ appear as negative terms in Eq. (3). The fraction $\lambda_z$ of the decayed compounds by inefficient osmoregulation still remains in the system as CR. The mineralization rates of DOC by these extracellular compounds is defined similarly to the uptake by fully operational cells,

$$C^{CR} = \underbrace{\mu_{CR}\chi_a\xi_c\overline{CR}}_{CR\ mineralization} \tag{39}$$

where $\mu_{CR}$ is the maximum specific mineralization rate by these cell residues. However, due to the nature of CR, C used by CR only contributes to respiration.

Substituting Eq. (24)–(39) into Eqs. (1)–(12), we obtain the following fully-parametrized form of the mass balance equations:

$$\frac{d\overline{POC}}{dt} = \underbrace{L}_{Litter\ input} \underbrace{-\left[1+m_d(1-\Gamma_s)\right]\nu_{POC}\chi_t\xi_{EE}\overline{POC}}_{POC\ decomposition} + \underbrace{(1-\lambda_r)\left[k_{AC}\overline{AC}+(1-\lambda_z)k_{AC}^s\chi_{os}^s\overline{AC}+k_{DC}\overline{DC}+k_{CR}\chi_a\overline{CR}+k_{EE}\theta_w\overline{EE}\right]}_{Recycling\ of\ decay\ products} \tag{40}$$

$$\frac{d(\theta_w\overline{DOC})}{dt} = \underbrace{\left[1+m_d(1-\Gamma_s)\right]\nu_{POC}\chi_t\xi_{EE}\overline{POC}}_{POC\ decomposition} - \underbrace{\mu_{AC}\chi_a\xi_c\overline{AC}}_{Uptake\ by\ AC} - \underbrace{\mu_{CR}\chi_a\xi_c\overline{CR}}_{Mineralization\ by\ CR} + \underbrace{\lambda_r\left[k_{AC}\overline{AC}+(1-\lambda_z)k_{AC}^s\chi_{os}^s\overline{AC}+k_{DC}\overline{DC}+k_{CR}\chi_a\overline{CR}+k_{EE}\theta_w\overline{EE}\right]}_{Recycling\ of\ decay\ products} -$$
$$\underbrace{z_r\tau_r\Gamma_m\xi_c\overline{DC}}_{Dormancy\ costs} + \underbrace{w_b\left(k_{AC}\overline{AC}+k_{AC}^s\chi_{os}^s\overline{AC}\right)\overline{OS_{AC}}+w_bk_{DC}\overline{DC}\,\overline{OS_{DC}}}_{Recycling\ of\ OS\ (cell\ decay)} + \underbrace{y_{os}\Pi_{os}\tau_{os}w_b\overline{AC}\left(\overline{OS_{AC}}-OS_{eq}^*\right)}_{Recycling\ of\ OS\ (osmoregulation)} - \underbrace{S^{DOC}}_{D/RW} \tag{41}$$

$$\frac{d\overline{AC}}{dt} = \underbrace{y^*(1-\lambda^*)\mu_{AC}\chi_a\xi_c\overline{AC}}_{AC\ synthesis} - \underbrace{\tau_i(1-\chi_a\xi_c)\overline{AC}}_{Inactivation} + \underbrace{\tau_r\Gamma_m\xi_c\overline{DC}}_{Reactivation} - \underbrace{(1-\Pi_{os})\tau_{os}w_b\overline{AC}\left(OS_{eq}^*-\overline{OS_{AC}}\right)}_{OS\ production} - \underbrace{k_{AC}\overline{AC}}_{AC\ natural\ decay} - \underbrace{k_{AC}^s\chi_{os}^s\overline{AC}}_{AC\ decay\ by\ stress} \tag{42}$$

$$\frac{d\overline{DC}}{dt} = \underbrace{\tau_i(1-\chi_a\xi_c)\overline{AC}}_{Inactivation} - \underbrace{\tau_r\Gamma_m\xi_c\overline{DC}}_{Reactivation} - \underbrace{k_{DC}\overline{DC}}_{DC\ decay} \tag{43}$$

$$\frac{d\overline{CR}}{dt} = \underbrace{\lambda_z k_{AC}^s\chi_{os}^s\overline{AC}}_{Osmolysis} - \underbrace{k_{CR}\chi_a\overline{CR}}_{CR\ decay} \tag{44}$$

$$\frac{d(\theta_w\overline{EE})}{dt} = \underbrace{y^*\lambda^*\mu_{AC}\chi_a\xi_c\overline{AC}}_{EE\ synthesis} - \underbrace{k_{EE}\theta_w\overline{EE}}_{EE\ decay} - \underbrace{S^{EE}}_{D/RW} \tag{45}$$

$$\frac{d(\theta_{AC}\overline{OS_{AC}})}{dt} = \underbrace{(1-\Pi_{os})\tau_{os}w_b\overline{AC}\left(OS_{eq}^*-\overline{OS_{AC}}\right)}_{OS\ production} - \underbrace{\Pi_{os}\tau_{os}w_b\overline{AC}\left(\overline{OS_{AC}}-OS_{eq}^*\right)}_{OS\ release\ (osmoregulation)} + \underbrace{w_b\overline{OS_{DC}}\tau_r\Gamma_m\xi_c\overline{DC}}_{OS\ reactivation} - \underbrace{w_b\overline{OS_{AC}}\tau_i(1-\chi_a\xi_c)\overline{AC}}_{OS\ inactivation} - \underbrace{w_b\overline{OS_{AC}}\left(k_{AC}\overline{AC}+k_{AC}^s\chi_{os}^s\overline{AC}\right)}_{OS\ release\ (AC\ decay)} \tag{46}$$

$$\frac{d(\theta_{DC}\overline{OS_{DC}})}{dt} = \underbrace{-w_b\overline{OS_{DC}}\tau_r\Gamma_m\xi_c\overline{DC}}_{OS\ reactivation} + \underbrace{w_b\overline{OS_{AC}}\tau_i(1-\chi_a\xi_c)\overline{AC}}_{OS\ inactivation} - \underbrace{w_b\overline{OS_{DC}}k_{DC}\overline{DC}}_{OS\ release\ (DC\ decay)} \tag{47}$$

Finally, the resulting equations for the fully-parametrized growth, respiration, and CUE are found as:

$$\text{Growth} = \underbrace{y^*\mu_{AC}\chi_a\xi_c\overline{AC}}_{Biomass\ synthesis} \tag{48}$$

$$\text{Respiration} = \underbrace{(1-y^*)\mu_{AC}\chi_a\xi_c\overline{AC}}_{Biomass\ synthesis\ costs} + \underbrace{\mu_{CR}\chi_a\xi_c\overline{CR}}_{Mineralization\ by\ CR} + \underbrace{(1-y_{os})\Pi_{os}\tau_{os}w_b\overline{AC}\left(\overline{OS_{AC}} - OS^*_{eq}\right)}_{Osmoregulation\ costs} + \underbrace{z_r\tau_r\Gamma_m\xi_c\overline{DC}}_{Dormancy\ costs} \tag{49}$$

$$\text{CUE} = \frac{\underbrace{y^*\mu_{AC}\chi_a\xi_c\overline{AC}}_{Biomass\ synthesis}}{\underbrace{\mu_{AC}\chi_a\xi_c\overline{AC}}_{Uptake\ by\ AC} + \underbrace{\mu_{CR}\chi_a\xi_c\overline{CR}}_{Mineralization\ by\ CR} + \underbrace{(1-y_{os})\Pi_{os}\tau_{os}\theta_{AC}\left(\overline{OS_{AC}} - OS^*_{eq}\right)}_{Osmoregulation\ costs} + \underbrace{z_r\tau_r\Gamma_m\xi_c\overline{DC}}_{Dormancy\ costs}} \tag{50}$$

## References


Allison, S.D., Goulden, M.L., 2017. Consequences of drought tolerance traits for microbial decomposition in the DEMENT model. Soil Biology and Biochemistry 107, 104–113. https://doi.org/10.1016/j.soilbio.2017.01.001.

Amato, P., Doyle, S.M., Battista, J.R., Christner, B.C., 2010. Implications of subzero metabolic activity on long-term microbial survival in terrestrial and extraterrestrial permafrost. Astrobiology. https://doi.org/10.1089/ast.2010.0477.

Archie, G.E., 1942. The electrical resistivity log as an aid in determining some reservoir characteristics. Transac. AIME. https://doi.org/10.2118/942054-G.

Barnard, R.L., Osborne, C.A., Firestone, M.K., 2015. Changing precipitation pattern alters soil microbial community response to wet-up under a Mediterranean-type climate. The ISME Journal 9, 946–957. https://doi.org/10.1038/ismej.2014.192.

Bauer, J., Herbst, M., Huisman, J.A., Weihermüller, L., Vereecken, H., 2008. Sensitivity of simulated soil heterotrophic respiration to temperature and moisture reduction functions. Geoderma 145, 17–27. https://doi.org/10.3987/REV-08-634.

Birch, H.F., 1958. The effect of soil drying on humus decomposition and nitrogen availability. Plant and Soil 10, 9–31. https://doi.org/10.1007/BF01343734.

Blagodatskaya, E., Kuzyakov, Y., 2013. Active microorganisms in soil: critical review of estimation criteria and approaches. Soil Biology and Biochemistry 67, 192–211. https://doi.org/10.1016/j.soilbio.2013.08.024.

Blazewicz, S.J., Schwartz, E., Firestone, M.K., 2014. Growth and death of bacteria and fungi underlie rainfall-induced carbon dioxide pulses from seasonally dried soil. Ecology 95, 1162–1172. https://doi.org/10.1890/13-1031.1.

Boot, C.M., Schaeffer, S.M., Schimel, J.P., 2013. Static osmolyte concentrations in microbial biomass during seasonal drought in a California grassland. Soil Biology and Biochemistry. https://doi.org/10.1016/j.soilbio.2012.09.005.

Brangarí, A.C.A.C., Fernàndez-Garcia, D., Sanchez-Vila, X., Manzoni, S., 2018. Ecological and soil hydraulic implications of microbial responses to stress - a modeling analysis. Advances in Water Resources 113, 178–194. https://doi.org/10.1016/j.advwatres.2017.11.005.

Carbone, M.S., Still, C.J., Ambrose, A.R., Dawson, T.E., Williams, A.P., Boot, C.M., Schaeffer, S.M., Schimel, J.P., 2011. Seasonal and episodic moisture controls on plant and microbial contributions to soil respiration. Oecologia 167, 265–278. https://doi.org/10.1007/s00442-011-1975-3.

Chapin, F.S., Matson, P.A., Mooney, H.A., 2002. Principles of terrestrial ecosystem ecology, principles of terrestrial ecosystem ecology. https://doi.org/10.1007/b97397.

Chase, F.E., Gray, P.H.H., 1957. Application of the Warburg respirometer in studying respiratory activity in soil. Canadian Journal of Microbiology. https://doi.org/10.1139/m57-038.

Chau, J., Bagtzoglou, A., Willig, M., 2011. The effect of soil texture on richness and diversity of bacterial communities. Environmental Forensics 12, 333–341. https://doi.org/10.1080/15275922.2011.622348.

Chowdhury, N., Yan, N., Islam, M.N., Marschner, P., 2011. The extent of drying influences the flush of respiration after rewetting in non-saline and saline soils. Soil Biology and Biochemistry. https://doi.org/10.1016/j.soilbio.2011.07.013.

de Nijs, E.A., Hicks, L.C., Leizeaga, A., Tietema, A., Rousk, J., 2018. Soil microbial moisture dependences and responses to drying-rewetting: the legacy of 18 years drought. Global Change Biology 1–11. https://doi.org/10.1111/gcb.14508.

De Nobili, M., Contin, M., Brookes, P.C., 2006. Microbial biomass dynamics in recently air-dried and rewetted soils compared to others stored air-dry for up to 103 years. Soil Biology and Biochemistry 38, 2871–2881. https://doi.org/10.1016/j.soilbio.2006.04.044.

Evans, S., Dieckmann, U., Franklin, O., Kaiser, C., 2016. Synergistic effects of diffusion and microbial physiology reproduce the Birch effect in a micro-scale model. Soil Biology and Biochemistry 93, 28–37. https://doi.org/10.1016/j.soilbio.2015.10.020.

Fierer, N., Schimel, J.P., 2003. A proposed mechanism for the pulse in carbon dioxide production commonly observed following the rapid rewetting of a dry soil. Soil Science Society of America Journal 67, 798. https://doi.org/10.2136/sssaj2003.0798.

Fierer, N., Schimel, J.P., 2002. Effects of drying-rewetting frequency on soil carbon and nitrogen transformations. Soil Biology and Biochemistry 34, 777–787. https://doi.org/10.1016/S0038-0717(02)00007-X.

Fischer, T., 2009. Substantial rewetting phenomena on soil respiration can be observed at low water availability. Soil Biology and Biochemistry 41, 1577–1579. https://doi.org/10.1016/j.soilbio.2009.04.009.

Flemming, H.-C., Wingender, J., 2010. The biofilm matrix. Nature Reviews Microbiology 8, 623–633. https://doi.org/10.1038/nrmicro2415.

Fraser, F.C., Corstanje, R., Deeks, L.K., Harris, J.A., Pawlett, M., Todman, L.C., Whitmore, A.P., Ritz, K., 2016. On the origin of carbon dioxide released from rewetted soils. Soil Biology and Biochemistry 101, 1–5. https://doi.org/10.1016/j.soilbio.2016.06.032.

Göransson, H., Godbold, D.L., Jones, D.L., Rousk, J., 2013. Bacterial growth and respiration responses upon rewetting dry forest soils: impact of drought-legacy. Soil Biology and Biochemistry 57, 477–486. https://doi.org/10.1016/j.soilbio.2012.08.031.

Griffiths, E., Birch, H.F., 1961. Microbiological changes in freshly moistened soil. Nature. https://doi.org/10.1038/189424a0.

Hamamoto, S., Moldrup, P., Kawamoto, K., Komatsu, T., 2010. Excluded-volume expansion of Archie's law for gas and solute diffusivities and electrical and thermal conductivities in variably saturated porous media. Water Resources Research 46, 1–14. https://doi.org/10.1029/2009WR008424.

Homyak, P.M., Blankinship, J.C., Slessarev, E.W., Schaeffer, S.M., Manzoni, S., Schimel, J.P., 2018. Effects of altered dry season length and plant inputs on soluble soil carbon. Ecology 99, 2348–2362. https://doi.org/10.1002/ecy.2473.

Iovieno, P., Bååth, E., 2008. Effect of drying and rewetting on bacterial growth rates in soil. FEMS Microbiology Ecology. https://doi.org/10.1111/j.1574-6941.2008.00524.x.

Jarvis, P., Rey, A., Petsikos, C., Wingate, L., Rayment, M., Pereira, J., Banza, J., David, J., Miglietta, F., Borghetti, M., Manca, G., Valentini, R., 2007. Drying and wetting of Mediterranean soils stimulates decomposition and carbon dioxide emission: the "Birch effect. Tree Physiology 27, 929–940. https://doi.org/10.1093/treephys/27.7.929.

Jenny, H., 1980. The soil resource, biology and fertility of soils. Ecological Studies. https://doi.org/10.1007/978-1-4612-6112-4. Springer New York, New York, NY.

Kakumanu, M.L., Cantrell, C.L., Williams, M.A., 2013. Microbial community reponse to varying magnitudes of desiccation in soil: a test of the osmolyte accumulation hypothesis. Soil Biology and Biochemistry 57, 644–653.

Kéraval, B., Catherine Lehours, A., Colombet, J., Amblard, C., Alvarez, G., Fontaine, S., 2016. Soil carbon dioxide emissions controlled by an extracellular oxidative metabolism identifiable by its isotope signature. Biogeosciences 13, 6353–6362. https://doi.org/10.5194/bg-13-6353-2016.

Kéraval, B., Fontaine, S., Lallement, A., Revaillot, S., Billard, H., Alvarez, G., Maestre, F., Amblard, C., Lehours, A.C., 2018. Cellular and non-cellular mineralization of organic carbon in soils with contrasted physicochemical properties. Soil Biology and Biochemistry 125, 286–289. https://doi.org/10.1016/j.soilbio.2018.07.023.

Khan, K.S., Mack, R., Castillo, X., Kaiser, M., Joergensen, R.G., 2016. Microbial biomass, fungal and bacterial residues, and their relationships to the soil organic matter C/N/P/S ratios. Geoderma. https://doi.org/10.1016/j.geoderma.2016.02.019.

Kieft, T.L., Soroker, E., Firestone, M.K., 1987. Microbial biomass response to a rapid increase in water potential when dry soil is wetted. Soil Biology and Biochemistry. https://doi.org/10.1016/0038-0717(87)90070-8.

Kim, D.G., Vargas, R., Bond-Lamberty, B., Turetsky, M.R., 2012. Effects of soil rewetting and thawing on soil gas fluxes: a review of current literature and suggestions for

future research. Biogeosciences 9, 2459–2483. https://doi.org/10.5194/bg-9-2459-2012.
Kirchman, D.L., 2013. Processes in microbial ecology, processes in microbial ecology. https://doi.org/10.1093/acprof:oso/9780199586936.001.0001.
Konopka, A., 2000. Theoretical analysis of the starvation response under substrate pulses. Microbial Ecology 38, 321–329. https://doi.org/10.1007/s002489900178.
Lado-Monserrat, L., Lull, C., Bautista, I., Lidón, A., Herrera, R., 2014. Soil moisture increment as a controlling variable of the "Birch effect". Interactions with the pre-wetting soil moisture and litter addition. Plant and Soil 379, 21–34. https://doi.org/10.1007/s11104-014-2037-5.
Lawrence, C.R., Neff, J.C., Schimel, J.P., 2009. Does adding microbial mechanisms of decomposition improve soil organic matter models? A comparison of four models using data from a pulsed rewetting experiment. Soil Biology and Biochemistry 41, 1923–1934. https://doi.org/10.1016/j.soilbio.2009.06.016.
Lee, X., Wu, H.J., Sigler, J., Oishi, C., Siccama, T., 2004. Rapid and transient response of soil respiration to rain. Global Change Biology. https://doi.org/10.1111/j.1529-8817.2003.00787.x.
Lennon, J.T., Jones, S.E., 2011. Microbial seed banks: the ecological and evolutionary implications of dormancy. Nature Reviews Microbiology 9, 119–130. https://doi.org/10.1038/nrmicro2504.
Li, X., Miller, A.E., Meixner, T., Schimel, J.P., Melack, J.M., Sickman, J.O., 2010. Adding an empirical factor to better represent the rewetting pulse mechanism in a soil biogeochemical model. Geoderma 159, 440–451. https://doi.org/10.1016/j.geoderma.2010.09.012.
Maggi, F., Porporato, A., 2007. Coupled moisture and microbial dynamics in unsaturated soils. Water Resources Research 43. https://doi.org/10.1029/2006WR005367.
Maire, V., Alvarez, G., Colombet, J., Comby, A., Despinasse, R., Dubreucq, E., Joly, M., Lehours, A.C., Perrier, V., Shahzad, T., Fontaine, S., 2013. An unknown oxidative metabolism substantially contributes to soil CO2 emissions. Biogeosciences 10, 1155–1167. https://doi.org/10.5194/bg-10-1155-2013.
Manzoni, S., Katul, G., 2014. Invariant soil water potential at zero microbial respiration explained by hydrological discontinuity in dry soils. Geophysical Research Letters 41, 7151–7158. https://doi.org/10.1002/2014GL061467.
Manzoni, S., Moyano, F., Kätterer, T., Schimel, J., 2016. Modeling coupled enzymatic and solute transport controls on decomposition in drying soils. Soil Biology and Biochemistry 95, 275–287. https://doi.org/10.1016/j.soilbio.2016.01.006.
Manzoni, S., Schaeffer, S.M., Katul, G., Porporato, A., Schimel, J.P., 2014. A theoretical analysis of microbial eco-physiological and diffusion limitations to carbon cycling in drying soils. Soil Biology and Biochemistry 73, 69–83. https://doi.org/10.1016/j.soilbio.2014.02.008.
Manzoni, S., Schimel, J.P., Porporato, A., 2012a. Responses of soil microbial communities to water stress: results from a meta-analysis. Ecology 93, 930–938. https://doi.org/10.1890/11-0026.1.
Manzoni, S., Taylor, P., Richter, A., Porporato, A., Ågren, G.I., 2012b. Environmental and stoichiometric controls on microbial carbon-use efficiency in soils. New Phytologist 196, 79–91. https://doi.org/10.1111/j.1469-8137.2012.04225.x.
Marschmann, G.L., Pagel, H., Kügler, P., Streck, T., 2019. Equifinality, sloppiness, and emergent structures of mechanistic soil biogeochemical models. Environmental Modelling & Software. https://doi.org/10.1016/j.envsoft.2019.104518.
Meisner, A., Bååth, E., Rousk, J., 2013. Microbial growth responses upon rewetting soil dried for four days or one year. Soil Biology and Biochemistry 66, 188–192. https://doi.org/10.1016/j.soilbio.2013.07.014.
Meisner, A., Leizeaga, A., Rousk, J., Bååth, E., 2017. Partial drying accelerates bacterial growth recovery to rewetting. Soil Biology and Biochemistry 112, 269–276. https://doi.org/10.1016/j.soilbio.2017.05.016.
Michaelis, L., Menten, M.L., 1913. Die kinetik der Invertinwirkung. Biochemische Zeitschrift. https://doi.org/10.1021/bi201284u.
Miller, A.E., Schimel, J.P., Meixner, T., Sickman, J.O., Melack, J.M., 2005. Episodic rewetting enhances carbon and nitrogen release from chaparral soils. Soil Biology and Biochemistry 37, 2195–2204. https://doi.org/10.1016/j.soilbio.2005.03.021.
Navarro-García, F., Casermeiro, M.Á., Schimel, J.P., 2012. When structure means conservation: effect of aggregate structure in controlling microbial responses to rewetting events. Soil Biology and Biochemistry. https://doi.org/10.1016/j.soilbio.2011.09.019.
Or, D., Phutane, S., Dechesne, A., 2007a. Extracellular polymeric substances affecting pore-scale hydrologic conditions for bacterial activity in unsaturated soils. Vadose Zone Journal 6, 298–305. https://doi.org/10.2136/vzj2006.0080.
Or, D., Smets, B.F., Wraith, J.M., Dechesne, A., Friedman, S.P., 2007b. Physical constraints affecting bacterial habitats and activity in unsaturated porous media - a review. Advances in Water Resources 30, 1505–1527. https://doi.org/10.1016/j.advwatres.2006.05.025.
Placella, S.A., Brodie, E.L., Firestone, M.K., 2012. Rainfall-induced carbon dioxide pulses result from sequential resuscitation of phylogenetically clustered microbial groups. Proceedings of the National Academy of Sciences 109, 10931–10936. https://doi.org/10.1073/pnas.1204306109.
Reichstein, M., Bahn, M., Ciais, P., Frank, D.C.D., Mahecha, M.D., Seneviratne, S.I., Zscheischler, J., Beer, C., Buchmann, N., Frank, .D.C.D., Papale, D., Rammig, A., Smith, P., Thonicke, K., van der Velde, M., Vicca, S., Walz, A., Wattenbach, M., 2013. Climate extremes and the carbon cycle. Nature 500, 287–295. https://doi.org/10.1038/nature12350.
Richards, L.A., Weaver, L.R., 1944. Moisture retention by some irrigated soils as related to soil-moisture tension. Journal of Agricultural Research 69, 215–235 citeulike-article-id:5774994.
Romaní, A.M., Fund, K., Artigas, J., Schwartz, T., Sabater, S., Obst, U., 2008. Relevance of polymeric matrix enzymes during biofilm formation. Microbial Ecology 56, 427–436. https://doi.org/10.1007/s00248-007-9361-8.
Rustad, L.E., Huntington, T.G., Boone, R.D., 2000. Controls on soil respiration: implications for climate change. Biogeochemistry 48, 1–6. https://doi.org/10.1023/A:1006255431298.
Salazar, A., Sulman, B.N., Dukes, J.S., 2018. Microbial dormancy promotes microbial biomass and respiration across pulses of drying-wetting stress. Soil Biology and Biochemistry 116, 237–244. https://doi.org/10.1016/j.soilbio.2017.10.017.
Schaeffer, S.M., Homyak, P.M., Boot, C.M., Roux-Michollet, D., Schimel, J.P., 2017. Soil carbon and nitrogen dynamics throughout the summer drought in a California annual grassland. Soil Biology and Biochemistry 115, 54–62. https://doi.org/10.1016/j.soilbio.2017.08.009.
Schimel, J., Balser, T.C., Wallenstein, M., 2007. Microbial stress-response physiology and its implications for ecosystem functioning. Ecology 88, 1386–1394. https://doi.org/10.1890/06-0219.
Schimel, J.P., 2018. Life in dry soils: effects of drought on soil microbial communities and processes. Annual Review of Ecology, Evolution and Systematics 49, 409–432. https://doi.org/10.1146/annurev-ecolsys-110617-062614.
Schimel, J.P., Schaeffer, S.M., 2012. Microbial control over carbon cycling in soil. Frontiers in Microbiology 3, 348. https://doi.org/10.3389/fmicb.2012.00348.
Schimel, J.P., Weintraub, M.N., 2003. The implications of exoenzyme activity on microbial carbon and nitrogen limitation in soil: a theoretical model. Soil Biology and Biochemistry 35, 549–563. https://doi.org/10.1016/S0038-0717(03)00015-4.
Schneider, M., Goss, K.-U., 2012. Prediction of water retention curves for dry soils from an established pedotransfer function: evaluation of the Webb model. Water Resources Research 48. https://doi.org/10.1029/2011WR011049.
Shi, A., Marschner, P., 2014. Drying and rewetting frequency influences cumulative respiration and its distribution over time in two soils with contrasting management. Soil Biology and Biochemistry. https://doi.org/10.1016/j.soilbio.2014.02.001.
Sierra, C.A., Trumbore, S.E., Davidson, E.A., Vicca, S., Janssens, I., 2015. Sensitivity of decomposition rates of soil organic matter with respect to simultaneous changes in temperature and moisture. Journal of Advances in Modeling Earth Systems 7, 335–356. https://doi.org/10.1002/2014MS000358.
Sleator, R.D., Hill, C., 2002. Bacterial osmoadaptation: the role of osmolytes in bacterial stress and virulence. FEMS Microbiology Reviews 26, 49–71. https://doi.org/10.1016/S0168-6445(01)00071-7.
Slessarev, E.W., Lin, Y., Jiménez, B.Y., Homyak, P.M., Chadwick, O.A., D'Antonio, C.M., Schimel, J.P., 2020. Cellular and extracellular C contributions to respiration after wetting dry soil. Biogeochemistry 147, 307–324. https://doi.org/10.1007/s10533-020-00645-y.
Slessarev, E.W., Schimel, J.P., 2020. Partitioning sources of CO2 emission after soil wetting using high-resolution observations and minimal models. Soil Biology and Biochemistry 143, 107753. https://doi.org/10.1016/j.soilbio.2020.107753.
Smith, B., Wärlind, D., Arneth, A., Hickler, T., Leadley, P., Siltberg, J., Zaehle, S., 2014. Implications of incorporating N cycling and N limitations on primary production in an individual-based dynamic vegetation model. Biogeosciences 11, 2027–2054. https://doi.org/10.5194/bg-11-2027-2014.
Stolpovsky, K., Martinez-Lavanchy, P., Heipieper, H.J., Van Cappellen, P., Thullner, M., 2011. Incorporating dormancy in dynamic microbial community models. Ecological Modelling 222, 3092–3102. https://doi.org/10.1016/j.ecolmodel.2011.07.006.
Sun, D., Li, K., Bi, Q., Zhu, J., Zhang, Q., Jin, C., Lu, L., Lin, X., 2017. Effects of organic amendment on soil aggregation and microbial community composition during drying-rewetting alternation. The Science of the Total Environment 574, 735–743. https://doi.org/10.1016/j.scitotenv.2016.09.112.
Tiemann, L.K., Billings, S.A., 2011. Changes in variability of soil moisture alter microbial community C and N resource use. Soil Biology and Biochemistry 43. https://doi.org/10.1016/j.soilbio.2011.04.020.
van Genuchten, M.T., 1980. A closed-form equation for predicting the hydraulic conductivity of unsaturated soils. Soil Science Society of America Journal 44.
Vetter, Y.A., Deming, J.W., Jumars, P.A., Krieger-Brockett, B.B., 1998. A predictive model of bacterial foraging by means of freely released extracellular enzymes. Microbial Ecology 36, 75–92. https://doi.org/10.1007/s002489900095.
Wang, G., Mayes, M.A., Gu, L., Schadt, C.W., 2014. Representation of dormant and active microbial dynamics for ecosystem modeling. PloS One. https://doi.org/10.1371/journal.pone.0089252.
Wang, G., Post, W.M., 2013. A note on the reverse Michaelis-Menten kinetics. Soil Biology and Biochemistry. https://doi.org/10.1016/j.soilbio.2012.08.028.
Warren, C.R., 2016. Do microbial osmolytes or extracellular depolymerisation products accumulate as soil dries? Soil Biology and Biochemistry 98, 54–63. https://doi.org/10.1016/j.soilbio.2016.03.021.
Webb, S.W., 2000. A simple extension of two-phase characteristic curves to include the dry region. Water Resources Research 36, 1425–1430. https://doi.org/10.1029/2000WR900057.
Williams, M.A., Xia, K., 2009. Characterization of the water soluble soil organic pool following the rewetting of dry soil in a drought-prone tallgrass prairie. Soil Biology and Biochemistry. https://doi.org/10.1016/j.soilbio.2008.08.013.
Wood, J.M., Bremer, E., Csonka, L.N., Kraemer, R., Poolman, B., Van der Heide, T., Smith, L.T., 2001. Osmosensing and osmoregulatory compatible solute accumulation by bacteria. Comparative Biochemistry and Physiology - A Molecular and Integrative Physiology. https://doi.org/10.1016/S1095-6433(01)00442-1.
Wu, J., Brookes, P.C., 2005. The proportional mineralisation of microbial biomass and organic matter caused by air-drying and rewetting of a grassland soil. Soil Biology and Biochemistry. https://doi.org/10.1016/j.soilbio.2004.07.043.
Wu, J.Q., Gui, S.X., Stahl, P., Zhang, R.D., 1997. Experimental study on the reduction of soil hydraulic conductivity by enhanced biomass growth. Soil Science 162, 741–748.
Xiang, S.R., Doyle, A., Holden, P.A., Schimel, J.P., 2008. Drying and rewetting effects on C and N mineralization and microbial activity in surface and subsurface California

grassland soils. Soil Biology and Biochemistry 40, 2281–2289. https://doi.org/10.1016/j.soilbio.2008.05.004.
Yarwood, R., Rockhold, M., Niemet, M., Selker, J., Bottomley, P., 2006. Impact of microbial growth on water flow and solute transport in unsaturated porous media. Water Resources Research 42. https://doi.org/10.1029/2005WR004550.
Yu, Z., Wang, G., Marschner, P., 2014. Drying and rewetting - effect of frequency of cycles and length ofmoist period on soil respiration and microbial biomass. European Journal of Soil Biology 62, 132–137. https://doi.org/10.1016/j.ejsobi.2014.03.007.
Zheng, Q., Hu, Y., Zhang, S., Noll, L., Böckle, T., Richter, A., Wanek, W., 2019. Growth explains microbial carbon use efficiency across soils differing in land use and geology. Soil Biology and Biochemistry 128, 45–55. https://doi.org/10.1016/j.soilbio.2018.10.006.